Reflectance spectroscopy allows rapid, accurate, and non-destructive estimates of functional traits from pressed leaves

Shan Kothari[1,2,4], Rosalie Beauchamp-Rioux[1], Etienne Laliberté[1], Jeannine Cavender-Bares[2,3]

[1]Institut de recherche en biologie végétale, Département de sciences biologiques, Université de Montréal, 4101 rue Sherbrooke Est, Montréal, QC, Canada H1X 2B2
[2]Department of Plant and Microbial Biology, University of Minnesota, 1479 Gortner Ave, St. Paul, MN, United States 55108
[3]Department of Ecology, Evolution, and Behavior, University of Minnesota, 1479 Gortner Ave, St. Paul, MN, United States 55108
[4]Corresponding author: shan.kothari@umontreal.ca

Running headline: Estimating traits from pressed-leaf spectra

Abstract

1. More than ever, ecologists seek to employ herbarium collections to estimate plant functional traits from the past and across biomes. However, many trait measurements are destructive, which may preclude their use on valuable specimens. Researchers increasingly use reflectance spectroscopy to estimate traits from fresh or ground leaves, and to delimit or identify taxa. Here, we extend this body of work to non-destructive measurements on pressed, intact leaves, like those in herbarium collections.
2. Using a dataset with 618 samples from 68 species, we used partial least-squares regression to build models linking pressed-leaf reflectance spectra to a broad suite of traits, including leaf mass per area (LMA), leaf dry matter content (LDMC), equivalent water thickness, carbon fractions, pigments, and twelve elements. We compared these models to those trained on fresh- or ground-leaf spectra of the same samples.
3. Our pressed-leaf models were best at estimating LMA (R^2 = 0.917; %RMSE = 7.30), C (R^2 = 0.774; %RMSE = 11.8), and N (R^2 = 0.772; %RMSE = 11.5), followed by water-related traits, carbon fractions, and pigments (all R^2 = 0.554-0.763; %RMSE = 12.3-18.6). Other than Ca, Na, and P, remaining elements were predicted poorly (R^2 < 0.5, %RMSE > 20). For most chemical traits, pressed-leaf models performed better than fresh-leaf models, but worse than ground-leaf models. Pressed-leaf models were worse than fresh-leaf models for estimating LMA and LDMC,

but better than ground-leaf models for LMA. Finally, in a subset of samples, we used partial least-squares discriminant analysis to classify specimens among 10 species with near-perfect accuracy from pressed- (>97%), and ground-leaf (>96%) spectra, and slightly lower accuracy from fresh-leaf spectra (>89%).

4. These results show that applying spectroscopy to pressed leaves is a promising way to estimate leaf functional traits and identify species without destructive analysis. Pressed-leaf spectra might combine advantages of fresh and ground leaves: like fresh leaves, they retain some of the spectral expression of leaf structure; but like ground leaves, they circumvent the masking effect of water absorption. Our study has far-reaching implications for capturing the wide range of functional and taxonomic information in the world's preserved plant collections.

Keywords: functional traits; herbarium collections; leaf chemistry; partial least-squares regression (PLSR); reflectance spectroscopy; species identification

Introduction

The world's herbaria together contain more than 390 million specimens (Thiers 2021) which are a rich source of information about global plant diversity. Herbarium specimens are collected for many reasons—often to document where a species is present, or to serve as vouchers for taxonomic studies. But these specimens are often repurposed for new ends, unforeseen by their collectors (Meineke et al. 2018). More than ever, ecologists and evolutionary biologists seek to use herbarium specimens to measure functional traits (Heberling 2021): for example, to evaluate the long-term imprint of human activity on plant communities (Lang et al. 2018; Meineke et al. 2018); to fill in gaps in sparse trait databases (Perez et al. 2020); or to conduct comparative studies of clades (Jardine et al. 2020). Measuring functional traits on herbarium specimens carries the promise of letting us reach the inaccessible, including the past or distant parts of the world. Using herbarium specimens also allows researchers to benefit from the expertise of taxonomists and refer back to the same specimens for further use—for example, as sources of genetic data, or as references for species identification from new collections (Heberling 2021). Using specimens, researchers can address ecological and evolutionary questions that require merging functional, genetic, and distributional data at global scales.

Many functional trait measurements require destructive sampling—for example, by grinding up tissue for chemical analyses. Such measurements include most protocols to determine the elemental or molecular composition of a sample (Pérez-Harguindeguy et al. 2013). Because herbarium specimens are irreplaceable—especially those from historical collections—curators may hesitate to let them be destroyed, even in part, for ecological research. Using specimens in functional ecology might be more feasible with new, non-destructive techniques to estimate their traits.

Reflectance spectroscopy is a technique often used to estimate foliar functional traits non-destructively (Curran 1989; Jacquemoud & Ustin 2020). A reflectance spectrum is a measurement of light's reflectance from a surface across a range of wavelengths; for leaf tissue, researchers tend to measure reflectance

between about 350 and 2500 nm, a range that includes over 98% of solar radiation reaching Earth's surface (American Society for Testing and Materials, 2006). Because the leaf's chemical and structural makeup determines how it absorbs, reflects, and transmits solar radiation, reflectance within this range carries information about many plant traits (Cavender-Bares et al. 2017).

Two main approaches exist to estimate traits from entire reflectance spectra. First, physics-based radiative transfer models like PROSPECT can be inverted to estimate a handful of traits with well-defined optical properties (Féret et al. 2017). Second, statistical models, often created using machine learning techniques like partial least-squares regression (PLSR), can estimate an even wider range of traits, albeit in a less mechanistic (and perhaps less general) way (Serbin & Townsend 2020). This multivariate empirical approach gives researchers the flexibility to predict complex traits whose absorption features might not be as strong or well-defined (Curran 1989). Likewise, multivariate classification techniques like partial least-squares discriminant analysis (PLS-DA) use the full spectrum to discriminate species, lineages, or other kinds of biological classes (Meireles et al. 2020b).

Empirical approaches like PLSR are widely used to estimate plant traits from spectroscopic data measured on fresh or ground leaves. These traits include leaf N and leaf mass per area (LMA; Asner et al. 2011; Serbin et al. 2014; Serbin et al. 2019; Streher et al. 2020), pigments (Asner et al. 2011; Yang et al. 2016), defense compounds (Couture et al. 2016; Nakaji et al. 2019), non-structural carbohydrates (Ely et al. 2019), and even photosynthetic capacity (Yan et al. 2021). Leaf-level PLSR models have been used to address such varied ecological topics as defense responses to herbivory (Kula et al. 2020) and the role of biodiversity in ecosystem function (Schweiger et al. 2018). Although this multivariate statistical approach is flexible, it is sensitive to the kind of leaf tissue used to train the model. Existing PLSR models have mostly been trained on reflectance spectra of fresh leaves (e.g. Serbin et al. 2019) or dried, ground leaves (e.g. Serbin et al. 2014). Such models are not expected to transfer to dried, intact leaves like herbarium specimens because both drying and grinding cause major changes in the spectrum.

We built PLSR models to estimate traits from the reflectance spectra of pressed leaves, like herbarium specimens, and compared their accuracy to models built from fresh or ground leaves. Costa et al. (2018) showed that a related spectroscopic technique, Fourier Transform-Near Infrared Spectroscopy (FT-NIR), could predict several leaf structural traits from pressed leaves of tropical trees. Here, we explicitly compare the accuracy of trait estimation from the spectra of fresh, pressed, and ground leaves for many leaf chemical and structural traits from multiple biomes and functional groups.

For most chemical traits, such as elemental composition or carbon fractions, we conjectured that ground-leaf spectral models would be the most accurate, as others have found (Serbin et al. 2014; Couture et al. 2016; Wang et al. 2020). Both drying and grinding might be important in achieving this accuracy. Drying may reveal minor absorption features of compounds in dry matter within the short-wave infrared (SWIR) range that, in fresh leaves, are obscured by the dominant effect of water absorption (Peterson et al. 1988). Grinding homogenizes the variation in structure and composition throughout the leaf lamina, which may allow us to capture a more even and representative sample of tissue (Richardson et al. 2021). Since pressed leaves are dried but not ground, we predicted they would yield intermediate accuracy for chemical traits.

For structural traits like LMA, we instead expected fresh and pressed leaves to outperform ground leaves because grinding disrupts the leaf structure. For water-related traits like leaf dry matter content (LDMC; dried mass divided by fresh mass), we expected fresh leaves to outperform both pressed and ground leaves because they retain the water absorption features that allow direct prediction of water content (Carter 1991). Likewise, because pigments tend to degrade after collection, we expected to estimate their concentration best from fresh leaves. We also assessed sample discoloration in preparation for mounting or in storage and considered whether it reduces the accuracy of trait estimates, which may indicate whether spectroscopy is useful on old or degraded specimens.

Finally, we asked whether pressed-leaf spectra can be used to identify samples to species. Reflectance spectra often show phylogenetic signal in certain wavelength ranges because of phylogenetic conservatism in their underlying traits (McManus et al. 2016; Meireles et al. 2020a; Diniz et al. 2020). This signal is what often makes it possible to classify species or higher-level taxa from fresh-leaf spectra (Cavender-Bares et al. 2016; Meireles et al. 2020b), but it may or may not be retained in pressed-leaf spectra. Studies with tropical forest species have demonstrated that FT-NIR absorbance spectra of pressed herbarium specimens can be used to classify species or higher-level taxa (Durgante et al. 2013; Lang et al. 2015; Prata et al. 2018). Based on these studies, Draper et al. (2020) proposed using spectra of herbarium specimens as part of an integrative process of species delimitation and identification. Here, we compare the accuracy of supervised classification from fresh-, pressed-, and ground-leaf spectra among the common species in our dataset. Because they preserve some of the leaf structure (unlike ground leaves) and reveal the distinctive SWIR absorption features of macromolecules and other compounds (unlike fresh leaves), pressed leaves may represent the best of both worlds for distinguishing species using spectroscopy.

Methods

Sampling

We trained PLSR models on leaf reflectance spectra and traits measured as part of four projects conducted by the Canadian Airborne Biodiversity Observatory (CABO). The projects are:

1. Beauchamp-Rioux: Deciduous forest trees sampled throughout the growing season in 2018 at several sites in southern Québec and Ontario (n = 405; 9 species).
2. Dessain: Forbs, grasses, shrubs, and broadleaf trees from forests and open areas sampled throughout the growing season in 2017 at four sites in southern Québec (n = 72; 59 species).
3. Boucherville: Forbs, shrubs, and grasses sampled throughout the growing season in 2018 from the Parc national des Îles-de-Boucherville in southern Québec (n = 73; 12 species).

4. Warren: A single broadleaf evergreen tree species (*Agonis flexuosa* (Willd.) Sweet) collected across a soil chronosequence (Turner et al. 2018) in southwestern Australia (n = 68).

The majority of samples were from trees (n = 504; 25 species), but herbs (n = 60; 19 species), shrubs (n = 48; 23 species), and vines (n = 6; 1 species) were also represented. The full sampling procedure is described in the Supplementary Materials. We validated the models both internally and on an independent dataset of pressed tree and herb samples collected at Cedar Creek Ecosystem Science Reserve (East Bethel, MN, USA).

Spectral and leaf trait measurements

For each CABO sample, we measured full-range reflectance spectra (350-2500 nm) of the leaves at three stages: (1) freshly sampled, (2) pressed and dried, and (3) ground into a fine powder. We measured fresh-leaf directional-hemispherical reflectance spectra on the adaxial surface of multiple leaves or leaf arrays from each sample using spectroradiometers equipped with integrating spheres. We pressed a portion of the sample, and measured reflectance spectra on the adaxial surface of pressed leaves between six months and three years later using a spectroradiometer with a leaf clip (Fig. S1). Lastly, we measured ground-leaf spectra using a spectroradiometer with a benchtop reflectance probe that pressed loose leaf powder into an even pellet with very low transmittance. We trimmed all spectra to 400-2400 nm. Detailed notes on measurement and post-measurement processing of reflectance spectra are found in the Supplementary Materials.

While measuring pressed-leaf spectra, we inspected each pressed specimen by eye to note signs of discoloration in preparation or storage. Typical forms of discoloration include blackening, browning, or the development of a silvery or whitish finish on the leaf surface. We scored each leaf on a discrete scale from 0 to 4. A score of 0 indicates no noticeable discoloration. Scores 1 through 4 indicate increasing discoloration, from 1 (either <5% blackening/browning or development of a slight silvery finish to the leaf) to 4 (>80% blackening/browning).

We measured the following leaf structural and chemical traits on each CABO sample: Leaf mass per area (LMA; kg m^{-2}), leaf dry matter content (LDMC; mg g^{-1}), equivalent water thickness (EWT; cm), carbon fractions (soluble cell contents, hemicellulose, cellulose, and lignin; %), pigments (chlorophyll *a*, chlorophyll *b*, and total carotenoids; mg g^{-1}), and concentrations of a variety of elements (Al, C, Ca, Cu, Fe, K, Mg, Mn, N, Na, P, Zn; % or mg g^{-1}). Protocol summaries are in the Supplementary Materials. We kept chemical traits on a mass basis for consistency with the usual basis on which such traits (except pigments) are measured and reported. However, some traits are most often distributed proportionally to area, and area-based retrievals may be better for some purposes (Kattenborn et al. 2019).

PLSR modeling for trait estimation

We used a PLSR modeling framework to predict each trait from each of fresh-, pressed-, and ground-leaf spectra across the full range (400-2400 nm). PLSR is suited to handle spectral datasets, which have many collinear predictors, because it projects the spectral matrix onto a smaller number of orthogonal latent components in a way that maximizes the ability to predict the response variable. We simply used reflectance values as predictors, since calculating various common transformations of reflectance (see Serbin et al. 2014) did not increase predictive accuracy in preliminary tests. We also did not transform any trait values to reduce skewness, again finding in preliminary tests that it did not improve predictive accuracy enough to warrant the added complexity. Some studies restrict the wavelengths used in prediction, often to ranges known or assumed to contain features relevant to a given trait (e.g. Serbin et al. 2014). Given that photosynthetic pigments could degrade and produce brown pigments in dry leaves (Fourty et al. 1996), we also built pressed-leaf models restricted to 1300-2400 nm, which might be expected to generalize better to datasets that include more degraded leaves. We present these results mainly in the Supplementary Materials.

Our methods for model calibration and validation largely follow Burnett et al. (2021). First, we randomly divided the data into calibration (75%) and validation (25%) datasets, stratified by project. We began by fitting a model for each trait on the calibration dataset. We selected the smallest number of components for which the root mean squared error of prediction (RMSEP) from 10-fold cross-validation fell within one standard deviation of the global minimum. We used this number of components—a different number for each trait—in further analyses to predict traits on the internal validation dataset. We calculated the variable importance in projection (VIP) metric for calibration models to see which parts of the spectrum were most important for predicting each trait (Wold et al. 1994).

To test how well we could predict traits on the internal validation subset, we first did a jackknife analysis by iteratively (100×) dividing the 75% calibration data further into random 70% training and 30% testing subsets. For each trait, we trained models on the 70% using the previously determined optimal number of components and predicted the remaining 30%. This analysis gave us a distribution of model performance statistics across the 100 iterates (R^2, %RMSE), which reveals the sensitivity of model performance to randomly varying sets of training and testing data.

Next, we applied the 100 jackknife models for each trait to the 25% internal validation dataset, yielding a distribution of 100 predictions for each validation sample. We quantified model performance using R^2 and root mean squared error (RMSE) between measurements and mean predictions. We also report the RMSE as a percentage of the 2.5% trimmed range (%RMSE), which we used rather than the full range (as in e.g. Burnett et al. 2021) for robustness to outliers. For each trait, we also tested whether the magnitude of residuals (observed minus predicted) in the validation dataset varied among leaves with different discoloration scores. We performed all statistical analyses in *R v. 3.6.3* (R Core Team 2020) and used package *pls v. 2.7.1* (Mevik et al. 2019) for PLSR modeling.

Finally, to test how well our model would transfer to a fully independent dataset, we applied the ensemble of pressed-leaf models for five traits (LMA, LDMC, EWT, N, and C) to pressed-leaf spectra from Cedar Creek, then compared the model-derived trait estimates to measured values. Like most of the CABO dataset, the Cedar Creek dataset comprises trees and herbs from northeastern temperate North America, but it includes an entire functional group (needleleaf conifers) absent among the CABO projects in this study. We collected the spectra with the same instrument and foreoptic as the pressed-leaf spectra in the CABO dataset, but used different sampling, preparation, and trait measurement protocols. Full details on this dataset are provided in Supplementary Materials.

PLS-DA modeling for species classification

We tested the potential to classify species with fresh-, pressed-, and ground-leaf spectra using partial least-squares discriminant analysis (PLS-DA; Barker & Rayens 2003). We took spectra from the ten most common species in our dataset—all of which are deciduous trees except *A. flexuosa*, which is evergreen. Each was represented by at least 20 specimens (~480 total). For each tissue type, we divided the full dataset into 60% calibration and 40% validation subsets. In the *R* library *caret v. 6.0.84* (Kuhn 2020), we trained models on the calibration subset using 10-fold cross-validation. We chose the number of PLS components during cross-validation by maximizing Cohen's kappa (κ), which describes the agreement between the true and predicted species identities while accounting for the probability of agreement by chance. Imbalanced training data can bias classification algorithms (Sun et al. 2009), so we used a two-step procedure to balance classes while maintaining enough training data and avoiding overfitting. First, we downsampled within better-represented species classes at random so that all classes had equal size, then chose the number of components (n) that maximized κ. Second, we upsampled from less-represented classes at random with replacement so that classes had equal size—again maximizing κ, but restricting the range of components evaluated to no more than the n chosen during the downsampling step. We applied the cross-validated PLS-DA model from the upsampling step to the validation subset and summarized its performance using raw classification accuracy and κ.

Results

Patterns in traits and reflectance spectra

We saw large variation among samples in each of our target traits, ranging from 1.4-fold variation in C to more than 20-fold variation in traits like lignin, P, K, and Zn (Table 1). The ranges of most traits in our dataset covered a large portion of the global distributions in the TRY dataset, but tended to be narrower at both extremes (Kattge et al. 2020). Trees tended to have higher LDMC, C, and lignin than other growth forms. Among the herbs, grasses had particularly high hemicellulose and cellulose and low lignin content, while forbs generally had high N. Some of the trait variation was driven by projects that occupied particular portions of trait space; for example, *A. flexuosa* in the Warren project tended to have particularly high LMA, Na, and C and low N.

Both pressed and ground leaves had higher median reflectance across nearly the entire spectrum (Fig. 1), as expected based on changes in water content and structure (Carter 1991). Indeed, water absorption features (the largest of which are centered around 1450 and 1930 nm) largely disappeared in pressed and ground leaves. The red edge between the visible and near-infrared (NIR) regions was also blunted by both pressing and grinding, causing the global maximum of median reflectance to shift from 872 nm (fresh) to 954 nm (pressed) to 1313 nm (ground). The coefficient of variation (CV) of reflectance was generally highest where average reflectance was lowest.

PLSR modeling for trait estimation

Tested on the internal validation dataset, pressed-leaf models performed best at predicting LMA (R^2 = 0.917; %RMSE = 7.30), C (R^2 = 0.774; %RMSE = 11.8), and N (R^2 = 0.772; %RMSE = 11.5). These traits were followed by a mixture of water-related traits, carbon fractions, and pigments, as well as Ca (all R^2 = 0.554-0.763; %RMSE = 12.3-18.6). Although some other elements (Na, P) could be estimated with $R^2 > 0.5$ and %RMSE < 20, most models for other elements showed lower accuracy (Table 1; Figs. 2-3

and S2-8). In most cases, the models restricted to 1300-2500 nm had slightly lower predictive accuracy than the full range models (Table S1).

We compared pressed-leaf models to both fresh-leaf and ground-leaf models. The optimal number of components selected to predict each trait was between 3 and 23. For any given trait, ground-leaf models always had the most components, usually followed by pressed-leaf models (Table 1). Fresh-leaf models were best for predicting the structural and water-related traits—LMA, LDMC, and EWT (Figs. 2-3 and S2-8). Ground-leaf models were best for predicting chemical traits, like carbon fractions and most elements. Fresh- and ground-leaf models had similar performance for pigments, both somewhat better than pressed-leaf models. Statistics from jackknife analyses showed that model performance was more variable for traits that were predicted less accurately (Figs. S9-11). There was no correlation between the magnitude of residuals and our discoloration index for any trait ($p > 0.05$).

For all traits except LMA and Fe, the VIP metric for fresh-leaf spectra showed a global maximum between 710 and 720 nm (Fig. 4 and S12-14)—wavelengths slightly longer than the typical inflection point of the red edge (Richardson et al. 2002). Many traits also show high VIP across the green hump at ~530-570 nm. Bands in the NIR range were less important for predicting most traits than much of the visible range. The SWIR range was generally important for predicting LMA, EWT, Na, and pigments, and many other traits showed several local peaks of importance, most prominently at about 1880 nm, but also near 1480 and 1720 nm.

For predicting traits from pressed-leaf spectra, the general trend held that visible reflectance and certain ranges in the SWIR were important for predicting most traits, while the NIR and much of the shorter SWIR (800-1750 nm) were less important (Fig. 4 and S12-14). The red edge peak of importance for most traits was near 705 nm. Other prominent local maxima for many traits lay close to 1440, 1720, 1920,

2130, and 2300 nm. We saw broadly similar patterns in ground-leaf spectra, except that VIP for most traits was lower at longer SWIR wavelengths (2000-2400 nm).

External validation

For most traits, pressed-leaf model performance on the external validation dataset from Cedar Creek was comparable to, but not quite as strong as, the internal validation (Table 2; Fig. 5). The exception was C, for which the models performed very poorly ($R^2 < 0.05$). Among the remaining traits, R^2 ranged from 0.557 (N) to 0.874 (LMA). For N in particular, %RMSE was high (37.8%) due to bias—N concentrations were underestimated for conifers but slightly overestimated for remaining samples.

Since conifers were absent from the CABO training dataset, we considered whether the models we built would extend to this new functional group. For N, models performed better when excluding conifers (R^2 = 0.594, %RMSE = 37.8) than when retaining them (R^2 = 0.557; %RMSE = 29.5). In contrast, for LMA, models performed worse when excluding conifers (R^2 = 0.762; %RMSE = 15.7) than when retaining them (R^2 = 0.874; %RMSE = 10.3), since their LMA values could be predicted well and extended the trait range. Models restricted to 1300-2500 nm did not consistently outperform those trained on the full range—they yielded somewhat better external validation R^2 for N, but worse for LDMC, both including and excluding conifers (Table S2; Fig. S15).

PLS-DA modeling for species classification

PLS-DA models using pressed- and ground-leaf spectra showed near-perfect performance at classifying species (Fig. 6). Models using fresh-leaf spectra were slightly worse but still showed strong performance. The optimal fresh-leaf model, which had 29 PLS components, correctly predicted the taxonomic identity of 170 of the 189 samples in the training dataset ($\kappa = 0.884$; $p < 0.0001$). The best pressed-leaf model, which had 29 PLS components, correctly predicted 184 of the 188 samples ($\kappa = 0.975$; $p < 0.0001$). The

best ground-leaf model, which had 30 PLS components, correctly predicted 183 out of 189 samples (κ = 0.963; $p < 0.0001$). In all cases, the majority (75-100%) of misclassifications were between congenerics.

Discussion

We show that we can estimate a wide range of leaf functional traits for 68 woody and herbaceous species from reflectance spectra of pressed leaves (Table 1; Figs. 2-3 and S2-8). Model performance was highest for LMA, C, and N, followed by a mixture of water-related traits, carbon fractions, pigments, and a few important elements (Ca, Na, and P). Other elements could only be estimated with fairly low accuracy. These results show that pressed-leaf spectra provide an integrative measure of leaf phenotypes, much like fresh-leaf spectra (Cavender-Bares et al. 2017), but with stronger potential to characterize variation in chemical traits. Perhaps as a result, we could use pressed-leaf spectra to classify species as accurately as ground-leaf spectra, and better than fresh-leaf spectra. Our results underscore the potential that using reflectance spectroscopy on herbarium specimens could yield rapid and non-destructive estimates of many functional traits, enabling more expansive studies of trait variation across space and time.

We compared pressed-leaf models to fresh-leaf and ground-leaf models from the same samples. Our findings about which kind of tissue was best for predicting each trait mostly supported our hypotheses. Ground-leaf spectra showed the strongest performance for chemical traits, likely because grinding homogenizes the lamina and removes the potentially confounding influence of leaf structure (Table 1). Pressed-leaf spectra showed intermediate performance for most chemical traits, perhaps because, like ground leaves, they lack the major water absorption features that mask the smaller features of other compounds in the SWIR range (Peterson et al. 1988). Contrary to our predictions, ground-leaf spectra performed about as well as fresh-leaf spectra, and better than pressed-leaf spectra, for estimating pigment concentrations. The same factors that provided an advantage to ground-leaf spectra in estimating chemical traits also perhaps explain why pressed- and (especially for LMA) ground-leaf spectra performed worse for estimating water-related and structural traits (LMA, LDMC, and EWT). Pressed-leaf models may

represent a good compromise in allowing many traits to be estimated with mostly intermediate but nonetheless quite high accuracy.

It may seem perplexing that we could succeed at all in predicting LMA from ground-leaf spectra, or LDMC and EWT from pressed- and ground-leaf spectra. The ability to estimate these traits must not result from the optical expression of the traits themselves. We suggest that we instead sense these traits via their correlations with other traits that have a stronger optical expression. This kind of effect—a "constellation effect" (*sensu* Chadwick & Asner 2016; Nunes et al. 2017)—has been invoked to explain the ability to estimate traits like rock-derived nutrients (Nunes et al. 2017) and $\delta^{15}N$ (Serbin et al. 2014) that are not known to have strong absorption features in the measured range of wavelengths. However, models that rely on such constellation effects could break down when patterns of trait covariance vary, which could make models for certain traits fail beyond the domain of the training data.

Our pressed-leaf models often performed as well as fresh- and ground-leaf models published here and elsewhere. For example, our models for LMA had an RMSE (0.0115 kg m^{-2}) lower than many fresh-leaf models from the literature, including Serbin et al. (2019; 0.015 kg m^{-2}), Nakaji et al. (2019; 0.015 kg m^{-2}), and Streher et al. (2020; 0.051 kg m^{-2}). The ground-leaf models in Serbin et al. (2014) had a validation RMSE of 1.4 and 2.4 for cellulose and lignin percentages, comparable to 1.52 and 2.30 for our pressed-leaf models (Table 1). On the other hand, Serbin et al. (2014)'s ground-leaf models for N performed better than our pressed-leaf models (2014; validation RMSE = 0.13 vs 0.273). Our models' error could be within acceptable bounds for addressing many questions about large-scale ecological or evolutionary patterns that encompass a wide range of trait variation. Moreover, our external validation analyses indicate that our models for some important traits—like LMA, LDMC, EWT, and N, but not C—can transfer reliably to other datasets.

The VIP metric helps us understand what features allow these models to work, but interpreting it can be challenging because reflectance at a given band is never driven by a single trait. Fresh-leaf VIP for most traits had peaks in the visible and SWIR ranges, with a global maximum at 705 nm (Fig. 4 and S12-14). The pattern of high VIP along the green hump and red edge is common in PLSR models from fresh leaves (Yang et al. 2016; Ely et al. 2019; Streher et al. 2020; Yan et al. 2021). The red edge (particularly 700-725 nm) may be so important because of its sensitivity to both chlorophyll content and leaf structure (Richardson et al. 2002). Much of the visible range was proportionally even more important for pressed- and ground-leaf models, and most of the NIR was less important (except for LMA; Fig. 4 and S12-14). There were multiple small VIP peaks in the SWIR. Although some (e.g. at 1440 and 1920 nm) lie within major water absorption features, any causal link to the leaf's fresh water content is unlikely for pressed and ground leaves. Many of these peaks also lie near broad absorption features for many components of dry matter, including protein, cellulose, lignin, and starch, which complicates their interpretation (Curran et al. 1989; Fourty et al. 1996).

With some exceptions, the VIP metric showed that the same bands are often important for predicting different traits. This pattern might be taken as an artifact of trait covariance: For example, the three pigment pools covaried strongly (R^2 = 0.827-0.969) and had nearly identical VIP across the spectrum (Figs. S12-14). One might take similarities in VIP further to imply that there are a small number of traits whose tight coordination with others underlies the performance of all models through constellation effects. Nevertheless, across the whole dataset, many traits covaried only weakly but still shared important VIP features. For example, EWT, cellulose, N, and K were not tightly coordinated (R^2 = 0.003-0.152) but shared similar patterns of pressed-leaf VIP across the spectrum (Fig. 4), including peaks at 705 and 1920 nm.

PLS-DA models showed that fresh-, pressed-, and ground-leaf spectra alike could be used to classify species with near-perfect accuracy (>96%) for pressed or ground leaves, and excellent (>89%) accuracy

for fresh leaves (Fig. 6). In contrast to prior work that deliberately selected many congenerics (Lang et al. 2015), our most common species were often distantly related. Among the misidentified samples, most were mistaken for congenerics, which implies that related species are more spectrally similar (Schweiger et al. 2018; Meireles et al 2020a). Hence, if we had included more closely related species, we might have seen a higher error rate. Nevertheless, our analysis reinforces that spectral models can often distinguish species or higher-level phylogenetic groups (Meireles et al. 2020b)—and that pressed- or ground-leaf models might be particularly suited to the task. We conjecture that these models have an advantage because drying reveals the absorption features of multiple compounds in the SWIR range that might together allow finer discrimination of species than water content. This result supports the growing practice of using spectra of pressed herbarium specimens in species delimitation and identification (Prata et al. 2018; Draper et al. 2020).

The future of spectroscopic trait estimation

Although trait predictions from spectral models are not perfect, they have a few advantages over conventional trait measurements: they (1) can be non-destructive; (2) are fast and require relatively little training; and (3) have very low marginal cost, despite the high capital cost of buying a spectrometer (Costa et al. 2018). These advantages could make it easier to address questions that require large datasets of functional traits. But researchers may be deterred if they must each build their own models tailored to particular uses—and for herbarium specimens, it might not be possible to do the destructive trait measurements often needed to train the models. Ideally, spectral models would be general enough that researchers could confidently use them without further validation, but this aim is not easy to achieve: for several reasons, a model trained on any particular spectral dataset may make poor trait predictions on new data. As with any other technique, the goal for spectroscopic trait estimation is to improve model accuracy and generality as much as they can be jointly improved. Below, we discuss some challenges one by one, particularly as they concern pressed leaves.

One concern is that the new data could be outside the range of traits or optical properties in the training dataset (Schweiger 2020). A general model, if such a thing is possible, would need to represent the full range of leaf functional traits and optical properties. Another kind of concern about model generality concerns sample preparation before spectral measurements. For example, particle size influences ground-leaf spectra (Foley et al. 1998). For pressed leaves, it may be particularly important to prepare samples in consistent ways that preserve the leaves' morphological integrity. In our external validation analyses, we found that pressed-leaf models yielded reasonably accurate predictions of most traits, even though the validation dataset differed in sample preparation protocols and included conifers, which were absent from the training dataset. Nevertheless, even setting aside conifers, external validation for one trait (C) was very poor, and for another (N) showed noticeable bias—enough that researchers might need to develop their own correction factors to use the model in practice.

Another class of challenges concerns spectrometers and their foreoptics. Spectra of fresh leaves can be measured with different foreoptics, including integrating spheres, contact probes, or leaf clips. We used a leaf clip with pressed specimens because mounting delicate pressed leaves in an integrating sphere could damage them. However, leaf clips and contact probes are less likely to produce consistent measurements among instruments or replicate samples due to variation in viewing geometry and anisotropic surface reflectance (Petibon et al. 2021). The logistical constraint of having to use a leaf clip or contact probe on pressed leaves could thus make it harder to compare data among instruments. Moreover, measuring reflectance with a leaf clip or probe usually requires placing a black absorbing background under the sample to keep transmitted light from being reflected back into the sensor, but many herbarium specimens are glued to a paper backing. When loose leaf material is not available, using spectra from these specimens may require new methods to correct for reflectance from the mounting paper.

Spectrometers and their software also vary subtly in their sensors and techniques for processing spectra (Castro-Esau et al. 2006), and in some cases researchers must take steps to reconcile spectra measured

from different instruments (Meireles et al. 2020b). Assuming that these kinds of technical challenges can be overcome, our results and others encourage confidence about building general models to estimate traits from a wide variety of plants (Serbin et al. 2019). The creation of open libraries for spectral data (like EcoSIS, https://ecosis.org/; or the CABO data portal, https://data.caboscience.org/leaf) and spectral models (like EcoSML; https://ecosml.org/) will contribute to this goal. Lastly, we note that many of the same concerns about discrepancies among sampling and measurement protocols could arise when using existing spectral libraries to aid in species identification (Draper et al. 2020).

What should herbarium managers do?

A particular challenge for herbarium specimens is that their optical and chemical properties may degrade during preparation or storage, especially light-sensitive pigments. Such degradation could make it hard to distinguish changes in the traits of living plants over time from changes in storage. Even in this study, where no specimens were collected before 2017, many underwent visible changes in color, including browning or blackening; ~12% were scored at 2 or higher. Certain preparation and storage conditions could accelerate changes in chemical or optical properties, including exposure to some chemical preservatives and high light, temperature, or humidity (Bridson & Forman 1999). Some species may also be more susceptible than others; in our dataset, ~42% of *Populus grandidentata* specimens were scored at 2 or higher, but no *Betula papyrifera* specimens were.

Whether such degradation could affect trait estimation is an open question. We find no evidence that it does, even for badly discolored specimens—but our specimens were collected no more than three years before measurement, while ecologists may want to use specimens collected decades ago. Long-term studies of specimens, perhaps subjected to varying preparation and storage techniques, could establish how optical properties change over time. In any case, estimating traits in old or degraded specimens will likely require including equally old or degraded specimens in the model training dataset.

Some of the challenges we describe pertain to projects that would measure spectra on samples already collected, but spectroscopy—among countless other novel uses for herbarium specimens—could also prompt changes in collection practice. For example, an herbarium could incorporate spectroscopy into its operations by measuring incoming specimens shortly after pressing, which could mitigate the challenges caused by mounting and degradation. Collecting and storing extra leaf material would also circumvent the challenge of measuring mounted leaves and aid other uses of herbarium specimens (Heberling 2021).

Collections-based research has been accelerated by advances in biodiversity informatics that make it easier to gather and synthesize data. If it becomes common to measure spectra on herbarium specimens—either during collection (fresh) or after (pressed)—linking spectral data to other specimen data may require new tools (Draper et al. 2020). The hyperdimensionality of the reflectance spectrum could make it hard to accommodate within existing standards like the Darwin Core (Wieczorek et al. 2012), at least without extensions. One could link records to external databases like EcoSIS or SPECCHIO (Hueni et al. 2020), which are also designed to store spectral metadata about instrumentation and processing. Coordination between herbarium managers and researchers who use reflectance spectroscopy could build agreement about best practices for measurement and curation.

We show that non-destructively measured pressed-leaf spectra retain much of the information about many leaf functional traits found in fresh-leaf spectra. While validating this technique on older specimens will require extensive further research, our findings suggest that reflectance spectroscopy could allow herbaria to take on a greater role in plant functional ecology and evolution. Our study has far-reaching implications for capturing the wide range of functional and phenotypic information in the world's preserved plant collections.

Acknowledgements

We performed this research on the ancestral and contemporary land—mostly unceded—of Native people: primarily the Kanien'kehá:ka (Mohawk), Omàmiwinini (Algonquin), and Abenaki First Nations for the Beauchamp-Rioux, Dessain, and Boucherville projects, the Noongar peoples for the Warren project, and the Dakota and Ojibwe peoples for the Cedar Creek dataset. For permissions and assistance, we thank the Jardin botanique de Montréal; la Station de biologie des Laurentides (SBL) de l'Université de Montréal; l'Institut de recherche d'Hydro-Québec (IREQ); the National Capital Commission for sampling at Mer Bleue Bog; la Société des établissements de plein air du Québec (SÉPAQ) for sampling at Parc national d'Oka, Parc national du Mont-Saint-Bruno, and Parc national des Îles-des-Boucherville; and the Parks and Wildlife Service of Western Australia for sampling in D'Entrecasteaux National Park. We thank Antoine Mathieu, Alexandra Massey, Florence Blanchard, Elisabeth Hardy-Lachance, Zachary Bélisle, Sandra Jooty, Myriam Cloutier, Fabien Cichonski, Madeleine Trickey-Massé, Vincent Fournier, Aurélie Dessain, Xavier Guilbeault-Mayers, Jocelyne Ayotte, Megan Erding, and especially Sabrina Demers-Thibeault for contributing to trait measurements. Carole Sinou, Phil Townsend, Dudu Meireles, Mason Heberling, and members of the Cavender-Bares lab and the Laboratory of Plant Functional Ecology (LEFO) contributed to insightful discussions. Data from Canadian and Australian sites were collected as part of the Canadian Airborne Biodiversity Observatory (CABO) funded by NSERC Discovery Frontiers grant 509190-2017, as well as NSERC Discovery grants (RGPIN-2014-06106, RGPIN-2019-04537) and a Canada Research Chair to EL. Cedar Creek collections were supported by the NSF/NASA (DEB-1342778) and the NSF ASCEND Biology Integration Institute (DBI-2021898). Cedar Creek is supported by the NSF Long-Term Ecological Research program, currently under DEB-1831944. Travel funding was provided by an International Thesis Research Travel Grant from the University of Minnesota's Graduate School and a grant distributed through an NSF-funded Research Coordination Network (DEB-1745562). SK was supported by an NSF Graduate Research Fellowship (Grant No. 00039202) and a UMN Doctoral Dissertation Fellowship. RBR was supported by NSERC through the Canada Graduate Scholarships—Master's program and the FRQNT through a Master's Research Scholarship.

Conflict of interest statement

The authors have no conflicts of interest to declare.

Author contributions

SK, JCB, and EL conceived the ideas and designed the methodology. RBR and SK collected the data. SK analyzed the data and wrote the first draft of the manuscript. All authors made substantial contributions to further drafts and gave final approval for publication.

Data availability

All fresh-leaf spectral data are available through the CABO data portal (https://data.caboscience.org/leaf). Upon publication, we will upload other spectral data, as well as metadata and trait data, to the Ecological Spectral Information System (EcoSIS, https://ecosis.org/), and upload models to the Ecological Spectral Model Library (EcoSML, https://ecosml.org/). At that stage, we will update this section accordingly.

Tables

Table 1: Summary statistics of PLSR model internal validations from fresh-, pressed-, and ground-leaf spectra. %RMSE is calculated as RMSE divided by the 2.5% trimmed range of data within the validation subset. Global ranges are derived from the TRY database (Kattge et al. 2020; accessed 13 April 2021), omitting data with error risk greater than 3. Carbon fractions (solubles, hemicellulose, cellulose, and lignin) and carotenoids are each represented by <1250 points in TRY, which may limit the estimates of the global range. EWT is not available on TRY.

			Fresh				Pressed				Ground			
Trait	Dataset range	Global range	No. comps	R^2	RMSE	%RMSE	No. comps	R^2	RMSE	%RMSE	No. comps	R^2	RMSE	%RMSE
LMA (kg m^{-2})	0.0233-0.217	0.00866-0.354	15	0.960	0.00795	5.05	9	0.917	0.0115	7.30	20	0.824	0.0165	10.5
LDMC (mg g^{-1})	155-573	68.2-857	16	0.853	26.0	8.82	17	0.713	36.4	12.3	20	0.764	33.1	11.2
EWT (cm)	0.00488-0.0282	NA	7	0.871	0.00167	9.99	14	0.763	0.00213	12.8	22	0.691	0.00242	14.5
Solubles (%)	38.5-88.9	20.0-74.6	15	0.438	6.12	19.5	12	0.701	4.31	13.6	23	0.814	3.36	10.6
Hemicellulose (%)	2.77-34.1	8.71-45.0	11	0.483	3.47	22.0	12	0.731	2.48	15.6	20	0.755	2.35	14.6
Cellulose (%)	5.19-25.8	7.65-42.6	20	0.482	2.29	27.4	15	0.735	1.52	18.1	21	0.872	1.04	12.4
Lignin (%)	0.918-21.5	2.27-32.4	10	0.497	2.42	19.6	12	0.554	2.30	18.6	20	0.777	1.65	13.3
C (%)	39.5-53.6	25.5-60.3	17	0.716	1.22	13.4	14	0.774	1.08	11.8	20	0.908	0.689	7.53
N (%)	0.883-5.62	0.14-7.27	10	0.729	0.301	12.6	15	0.772	0.273	11.5	22	0.952	0.127	5.31
Chl *a* (mg g^{-1})	1.24-15.5	1.38-22.1 (total Chl)	5	0.719	1.12	14.1	7	0.626	1.30	16.4	9	0.719	1.14	14.4
Chl *b* (mg g^{-1})	0.486-5.29		5	0.696	0.397	14.7	6	0.555	0.484	17.9	8	0.688	0.410	15.2
Carotenoids (mg g^{-1})	0.193-3.05	0.00102-5.1	5	0.638	0.264	16.9	7	0.615	0.274	17.5	16	0.712	0.240	15.3
Al (mg g^{-1})	0-0.379	0.004-19.7	5	0.220	0.0415	24.5	6	0.243	0.0409	24.1	10	0.593	0.0304	17.9
Ca (mg g^{-1})	1.64-36.9	0.68-69	11	0.425	5.34	19.0	17	0.744	3.57	12.7	23	0.868	2.58	9.16
Cu (mg g^{-1})	0-0.052	0.00154-0.064	8	0.472	0.00577	20.6	10	0.301	0.00653	23.2	7	0.340	0.00641	23.1
Fe (mg g^{-1})	0.0150-0.266	0.0128-1.1	4	0.267	0.0380	20.4	7	0.215	0.0392	21.0	9	0.358	0.0356	19.1
K (mg g^{-1})	1.06-38.2	0.3-78.1	7	0.598	2.92	17.6	14	0.488	3.18	20.1	17	0.694	2.55	15.3
Mg (mg g^{-1})	0.482-7.86	0.277-15.6	7	0.253	0.802	22.1	13	0.373	0.759	20.9	23	0.529	0.656	18.0
Mn (mg g^{-1})	0-1.02	0.00560-5.37	3	0.198	0.158	25.3	12	0.349	0.144	22.9	17	0.655	0.107	18.1
Na (mg g^{-1})	0-4.87	0.00499-48.7	4	0.360	0.612	21.9	9	0.514	0.537	19.2	14	0.426	0.579	20.7

P (mg g^{-1})	0.222-7.18	0.1-9.9	7	0.389	0.866	21.3	19	0.547	0.738	18.1	13	0.598	0.699	17.2
Zn (mg g^{-1})	0.00142-0.647	0.00221-0.242	9	0.250	0.0744	26.2	8	0.310	0.0704	24.8	15	0.437	0.0634	22.3

Table 2: Summary statistics for external validation of pressed-leaf PLSR models. The models were trained on CABO data (see Table 1) and applied to a dataset collected at Cedar Creek.

	Including conifers				Excluding conifers			
Trait	Range	R^2	RMSE	%RMSE	Range	R^2	RMSE	%RMSE
LMA (kg m^{-2})	0.0179-0.229	0.874	0.0186	10.3	0.0179-0.136	0.762	0.0126	15.7
LDMC (mg g^{-1})	133-525	0.559	47.8	16.9	133-504	0.571	49.7	17.2
EWT (cm)	0.00602-0.0372	0.609	0.00449	18.1	0.00602-0.0363	0.567	0.00354	19.6
C (%)	35.7-59.8	0.033	4.42	25.2	35.7-54.1	0.036	4.21	27.1
N (%)	0.75-4.68	0.557	0.725	37.8	0.75-4.68	0.594	0.754	29.5

Figures

Fig. 1: Distributions of spectral reflectance and its coefficient of variation (CV) among fresh (A), pressed (B), and ground (C) leaf samples. A solid black line connects the median reflectance at each wavelength. Dark blue and light blue ribbons denote the middle 50% and 95%. The solid red line shows the coefficient of variation at each wavelength.

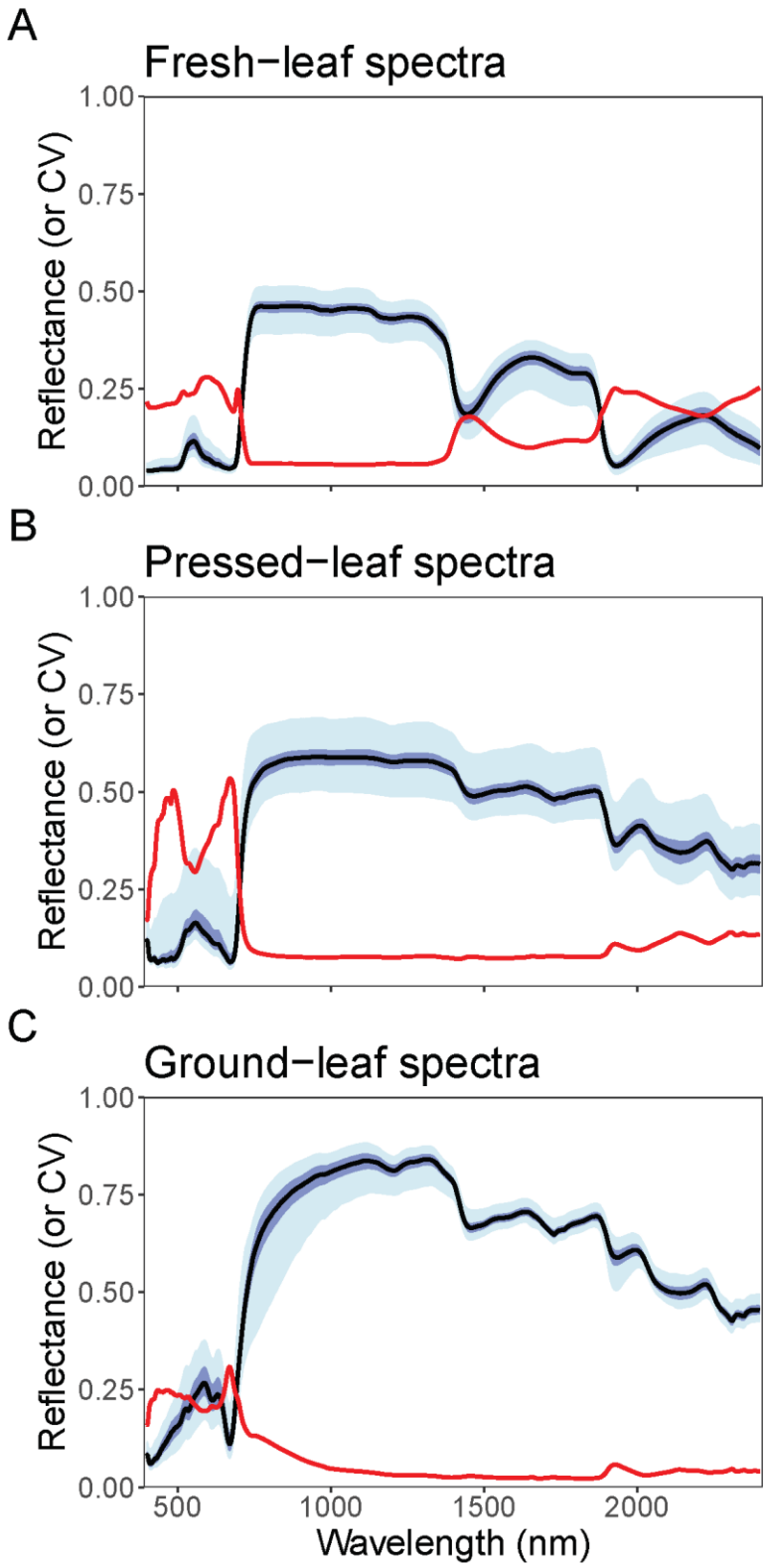

Fig. 2: Internal validation results for LMA, EWT, cellulose, and chlorophyll *a* predicted from fresh- (left), pressed- (middle), and ground-leaf (right) spectra. In each panel, each functional group has a separate ordinary least-squares regression line overlaid on top of the thick dashed 1:1 line. The error bars for each data point are 95% confidence intervals calculated from the distribution of predictions based on the ensemble of 100 models produced from jackknife analyses. Figs. 2 and 3 display a subset of traits that represent various functions and span the range of model performance. Plots for remaining traits are in the Supplementary Materials.

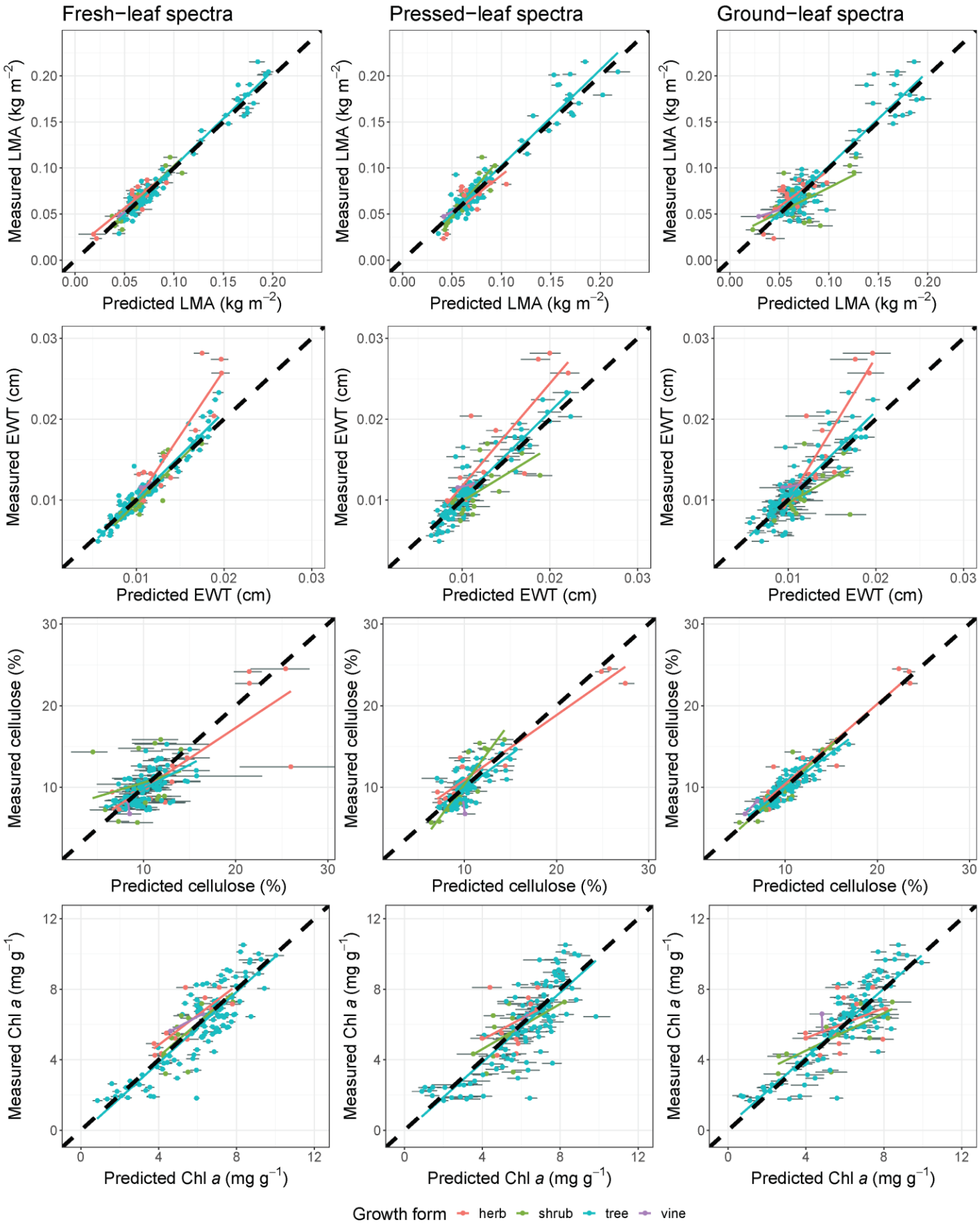
Fresh−leaf spectra
Pressed−leaf spectra
Ground−leaf spectra
Measured LMA (kg m−2)
Predicted LMA (kg m−2)
Measured EWT (cm)
Predicted EWT (cm)
Measured cellulose (%)
Predicted cellulose (%)
Measured Chl a (mg g−1)
Predicted Chl a (mg g−1)
Growth form
herb
shrub
tree
vine

566

Fig. 3: Internal validation results for three elements (N, K, and Mn) predicted from fresh- (left), pressed- (middle), and ground-leaf (right) spectra, displayed as in Fig. 2.

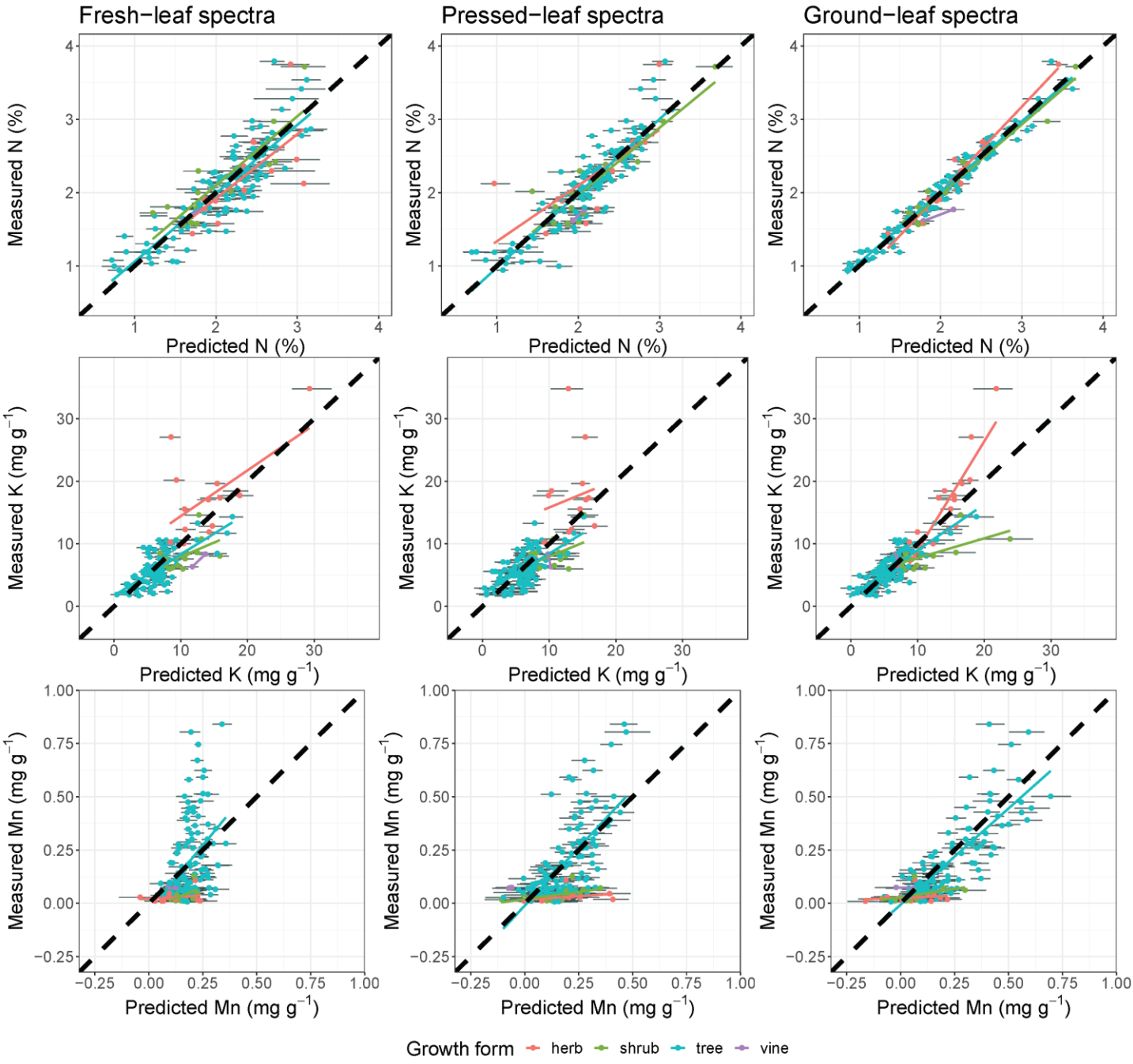

Fig. 4: The variable importance of projection (VIP) metric calculated based on fresh- (left), pressed- (middle), and ground-leaf (right) models. As in Figs. 2 and 3, we selected seven traits that represent a range of patterns in VIP across the tissue types (cell = cellulose). The dashed horizontal line at 0.8 represents a heuristic threshold for importance suggested by Burnett et al. (2021). VIP plots for remaining traits are in the Supplementary Materials.

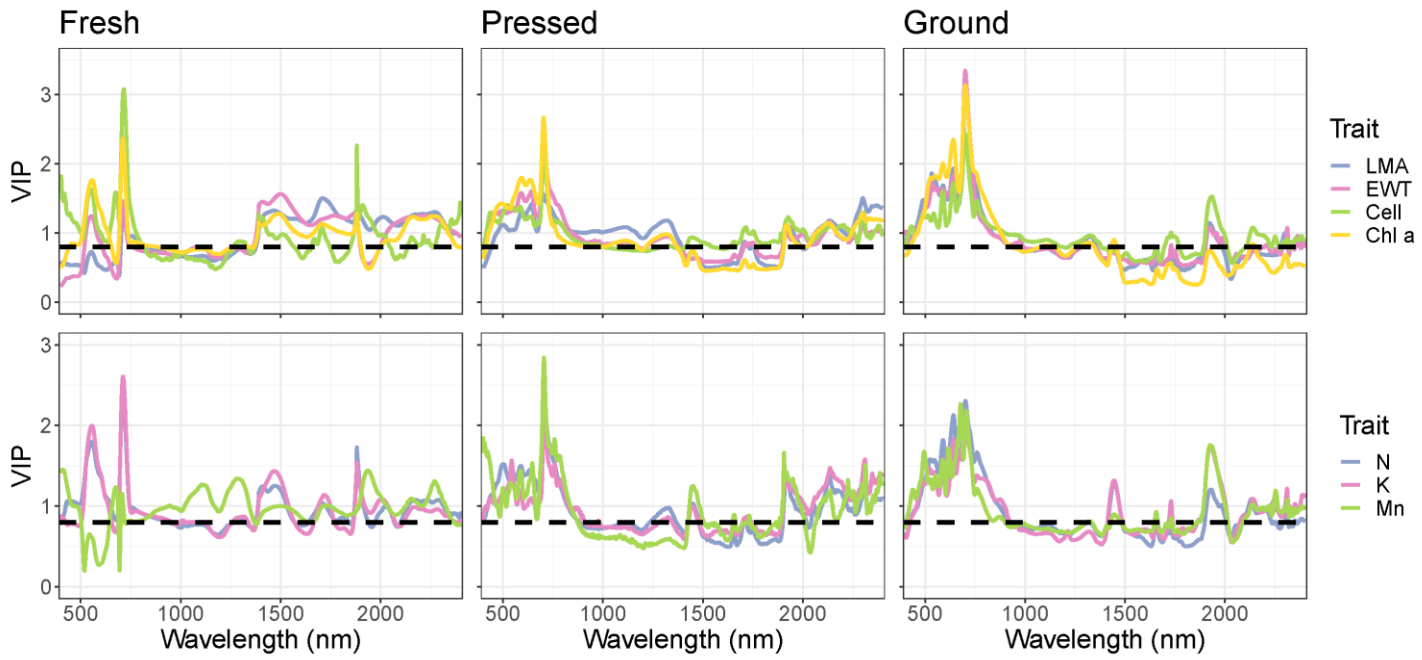

Fig. 5: External validation results for various traits in Cedar Creek data predicted using models trained on CABO data. Panels are displayed as in Figs. 2 and 3.

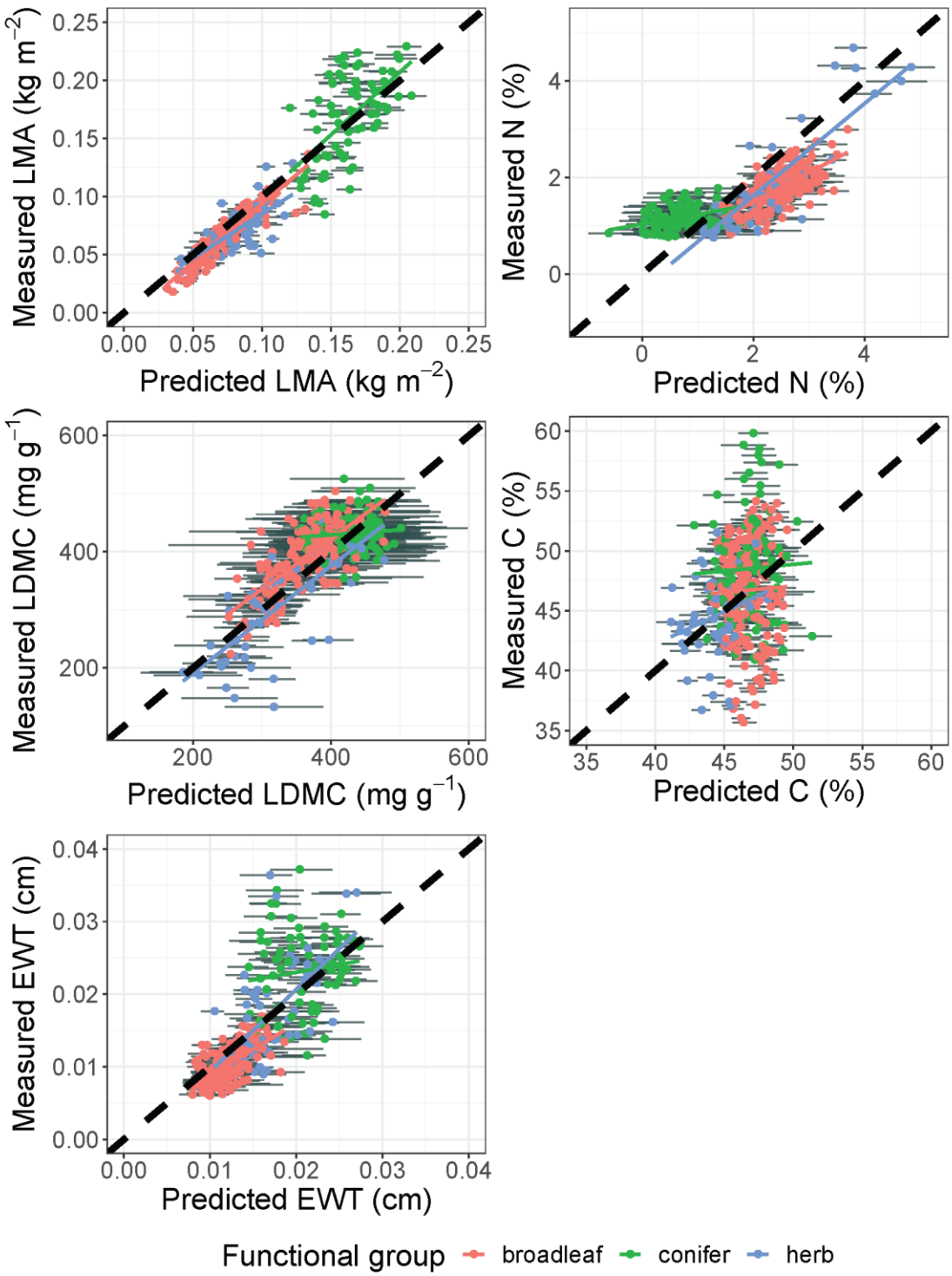

Fig. 6: Confusion matrices for partial least-squares discriminant analysis from (A) fresh-, (B) pressed-, and (C) ground-leaf spectra. Rows specify the true species identity, while columns specify the models' predictions. Numbers on the diagonal represent specimens correctly classified, while off-diagonals represent those misclassified. Full binomials: *Agonis flexuosa*, *Acer rubrum* L., *A. saccharinum* L., *A. saccharum* Marshall, *Betula papyrifera* Marshall, *B. populifolia* Marshall, *Fagus grandifolia* Ehrh., *Populus grandidentata* Michx., *Populus tremuloides* Michx., and *Quercus rubra* L.

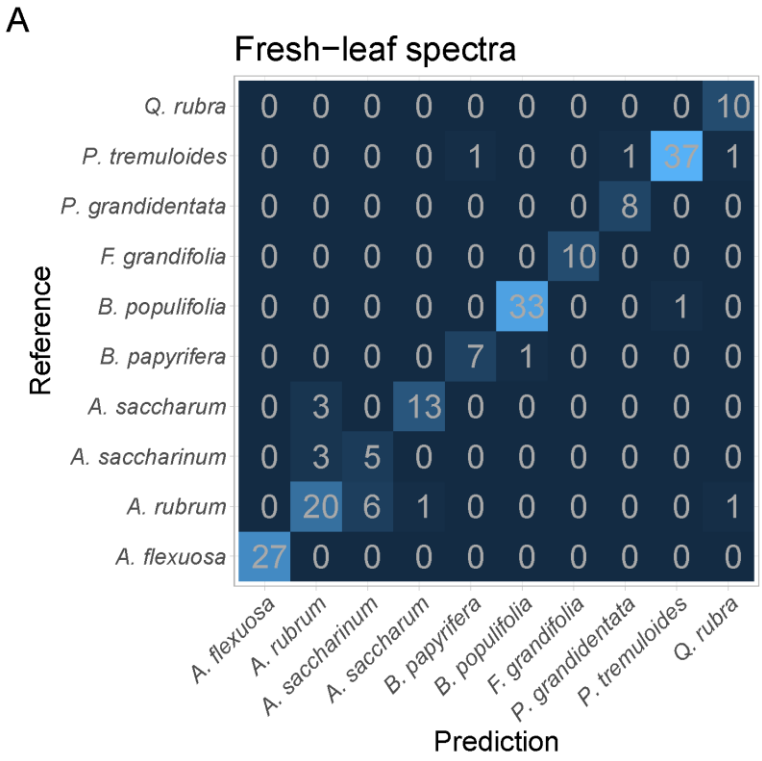

B

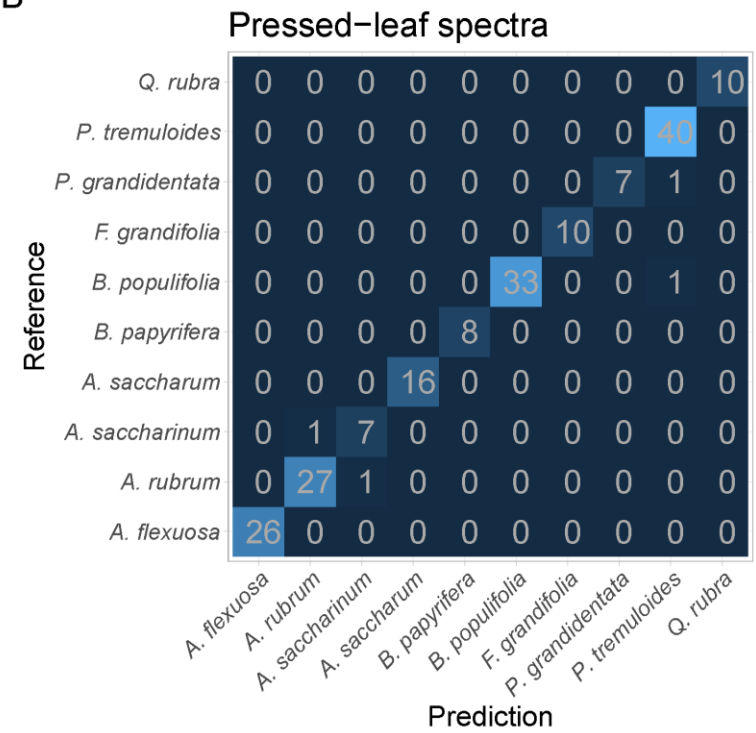
Pressed−leaf spectra
Reference
Prediction
Q. rubra 0 0 0 0 0 0 0 0 0 10
P. tremuloides 0 0 0 0 0 0 0 0 40 0
P. grandidentata 0 0 0 0 0 0 0 7 1 0
F. grandifolia 0 0 0 0 0 0 10 0 0 0
B. populifolia 0 0 0 0 0 33 0 0 1 0
B. papyrifera 0 0 0 0 8 0 0 0 0 0
A. saccharum 0 0 0 16 0 0 0 0 0 0
A. saccharinum 0 1 7 0 0 0 0 0 0 0
A. rubrum 0 27 1 0 0 0 0 0 0 0
A. flexuosa 26 0 0 0 0 0 0 0 0 0
A. flexuosa
A. rubrum
A. saccharinum
A. saccharum
B. papyrifera
B. populifolia
F. grandifolia
P. grandidentata
P. tremuloides
Q. rubra

607

C

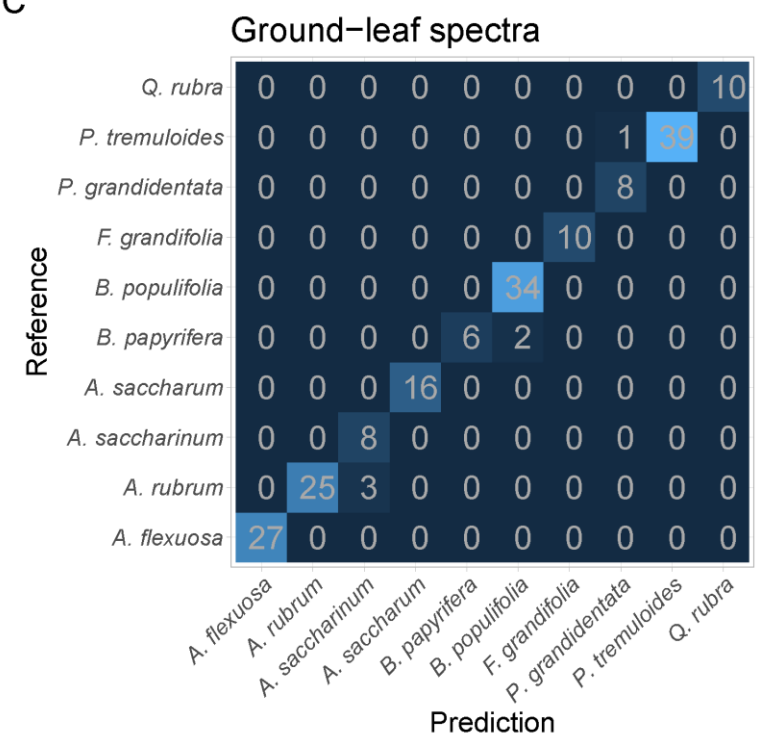
Ground−leaf spectra
Reference
Prediction
Q. rubra 0 0 0 0 0 0 0 0 0 10
P. tremuloides 0 0 0 0 0 0 0 1 39 0
P. grandidentata 0 0 0 0 0 0 0 8 0 0
F. grandifolia 0 0 0 0 0 0 10 0 0 0
B. populifolia 0 0 0 0 0 34 0 0 0 0
B. papyrifera 0 0 0 0 6 2 0 0 0 0
A. saccharum 0 0 0 16 0 0 0 0 0 0
A. saccharinum 0 0 8 0 0 0 0 0 0 0
A. rubrum 0 25 3 0 0 0 0 0 0 0
A. flexuosa 27 0 0 0 0 0 0 0 0 0
A. flexuosa
A. rubrum
A. saccharinum
A. saccharum
B. papyrifera
B. populifolia
F. grandifolia
P. grandidentata
P. tremuloides
Q. rubra

608

References

American Society for Testing and Materials. (2006). *Standard Tables for Reference Solar Spectral Irradiances: Direct Normal and Hemispherical on 37° Tilted Surface* (Standard G173-06).

Asner, G. P., Martin, R. E., Knapp, D. E., Tupayachi, R., Anderson, C., Carranza, L., Martinez, P., Houcheime, M., Sinca, F., & Weiss, P. (2011). Spectroscopy of canopy chemicals in humid tropical forests. *Remote Sensing of Environment, 115*(12), 3587–3598.

Barker, M., & Rayens, W. (2003). Partial least squares for discrimination. *Journal of Chemometrics*, 17(3), 166–173.

Bridson, D. & Forman, L. (1999). The Herbarium Handbook. Royal Botanic Gardens, Kew, Richmond U.K.

Burnett, A. C., Anderson, J., Davidson, K. J., Ely, K. S., Lamour, J., Li, Q., Morrison, B. D., Yang, D., Rogers, A., & Serbin, S. P. (2021). A best-practice guide to predicting plant traits from leaf-level hyperspectral data using partial least squares regression. *Journal of Experimental Botany*, erab295.

Carter, G. A. (1991). Primary and Secondary Effects of Water Content on the Spectral Reflectance of Leaves. *American Journal of Botany*, *78*(7), 916–924.

Castro-Esau, K. L., Sánchez-Azofeifa, G. A., & Rivard, B. (2006). Comparison of spectral indices obtained using multiple spectroradiometers. *Remote Sensing of Environment, 103*(3), 276–288.

Cavender-Bares, J., Gamon, J. A., Hobbie, S. E., Madritch, M. D., Meireles, J. E., Schweiger, A. K., & Townsend, P. A. (2017). Harnessing plant spectra to integrate the biodiversity sciences across biological and spatial scales. *American Journal of Botany, 104*(7), 966–969.

Cavender-Bares, J., Meireles, J. E., Couture, J. J., Kaproth, M. A., Kingdon, C. C., Singh, A., Serbin, S. P., Center, A., Zuniga, E., Pilz, G., & Townsend, P. A. (2016). Associations of Leaf Spectra with Genetic and Phylogenetic Variation in Oaks: Prospects for Remote Detection of Biodiversity. *Remote Sensing, 8*(3), 221.

Chadwick, K. D., & Asner, G. P. (2016). Organismic-Scale Remote Sensing of Canopy Foliar Traits in Lowland Tropical Forests. *Remote Sensing, 8*(2), 87.

Costa, F. R. C., Lang, C., Almeida, D. R. A., Castilho, C. V., & Poorter, L. (2018). Near-infrared spectrometry allows fast and extensive predictions of functional traits from dry leaves and branches. *Ecological Applications, 28*(5), 1157–1167.

Couture, J. J., Singh, A., Rubert-Nason, K. F., Serbin, S. P., Lindroth, R. L., & Townsend, P. A. (2016). Spectroscopic determination of ecologically relevant plant secondary metabolites. *Methods in Ecology and Evolution, 7*(11), 1402–1412.

Curran, P. J. (1989). Remote sensing of foliar chemistry. *Remote Sensing of Environment, 30*(3), 271–278.

Diniz, É. S., Amaral, C. H., Sardinha, S. T., Thiele, J., & Meira-Neto, J. A. A. (2020). Phylogenetic signatures in reflected foliar spectra of regenerating plants in Neotropical forest gaps. *Remote Sensing of Environment*, 112172.

Draper, F. C., Baker, T. R., Baraloto, C., Chave, J., Costa, F., Martin, R. E., Pennington, R. T., Vicentini, A., & Asner, G. P. (2020). Quantifying Tropical Plant Diversity Requires an Integrated Technological Approach. *Trends in Ecology & Evolution, 35*(12), 1100–1109.

Durgante, F. M., Higuchi, N., Almeida, A., & Vicentini, A. (2013). Species Spectral Signature: Discriminating closely related plant species in the Amazon with Near-Infrared Leaf-Spectroscopy. *Forest Ecology and Management, 291*, 240–248.

Ely, K. S., Burnett, A. C., Lieberman-Cribbin, W., Serbin, S. P., & Rogers, A. (2019). Spectroscopy can predict key leaf traits associated with source–sink balance and carbon–nitrogen status. *Journal of Experimental Botany, 70*(6), 1789–1799.

Féret, J.-B., Gitelson, A. A., Noble, S. D., & Jacquemoud, S. (2017). PROSPECT-D: Towards modeling leaf optical properties through a complete lifecycle. *Remote Sensing of Environment, 193*, 204–215.

Foley, W. J., McIlwee, A., Lawler, I., Aragones, L., Woolnough, A. P., & Berding, N. (1998). Ecological applications of near infrared reflectance spectroscopy – a tool for rapid, cost-effective prediction of the composition of plant and animal tissues and aspects of animal performance. *Oecologia, 116*(3), 293–305.

Fourty, Th., Baret, F., Jacquemoud, S., Schmuck, G., & Verdebout, J. (1996). Leaf optical properties with explicit description of its biochemical composition: Direct and inverse problems. *Remote Sensing of Environment, 56*(2), 104–117.

Heberling, J. M. (2021). Herbaria as Big Data Sources of Plant Traits. *International Journal of Plant Sciences*. (in press)

Hueni, A., Chisholm, L. A., Ong, C., Malthus, T. J., Wyatt, M., Trim, S. A., Schaepman, M. E., & Thankappan, M. (2020). The SPECCHIO Spectral Information System. *IEEE Journal of Selected Topics in Applied Earth Observations and Remote Sensing*, 13, 5789–5799.

Jacquemoud, S., & Ustin, S. (2019). Leaf Optical Properties. Cambridge University Press, New York.

Jardine, E. C., Thomas, G. H., Forrestel, E. J., Lehmann, C. E. R., & Osborne, C. P. (2020). The global distribution of grass functional traits within grassy biomes. *Journal of Biogeography*, *47*(3), 553–565.

Kattenborn, T., Schiefer, F., Zarco-Tejada, P., & Schmidtlein, S. (2019). Advantages of retrieving pigment content [µg/cm2] versus concentration [%] from canopy reflectance. *Remote Sensing of Environment*, 230, 111195.

Kattge, J., Bönisch, G., Díaz, S., Lavorel, S., Prentice, I. C., Leadley, P., Tautenhahn, S., Werner, G. D. A., Aakala, T., Abedi, M., et al. (2020). TRY plant trait database – enhanced coverage and open access. *Global Change Biology*, *26*(1), 119–188.

Kuhn, M. (2020). caret: Classification and Regression Training. R package version 6.0-86. https://CRAN.R-project.org/package=caret

Kula, A. A. R., Hey, M. H., Couture, J. J., Townsend, P. A., & Dalgleish, H. J. (2020). Intraspecific competition reduces plant size and quality and damage severity increases defense responses in the herbaceous perennial, *Asclepias syriaca*. *Plant Ecology*, *221*(6), 421–430.

Lang, C., Costa, F. R. C., Camargo, J. L. C., Durgante, F. M., & Vicentini, A. (2015). Near Infrared Spectroscopy Facilitates Rapid Identification of Both Young and Mature Amazonian Tree Species. *PLOS ONE*, *10*(8), e0134521.

Lang, P. L. M., Willems, F. M., Scheepens, J. F., Burbano, H. A., & Bossdorf, O. (2019). Using herbaria to study global environmental change. *New Phytologist*, *221*(1), 110–122.

McManus, K. M., Asner, G. P., Martin, R. E., Dexter, K. G., Kress, W. J., & Field, C. B. (2016). Phylogenetic Structure of Foliar Spectral Traits in Tropical Forest Canopies. *Remote Sensing*, *8*(3), 196.

Meineke, E. K., Davis, C. C., & Davies, T. J. (2018). The unrealized potential of herbaria for global change biology. *Ecological Monographs*, *88*(4), 505–525.

Meireles, J. E., B. O'Meara, and J. Cavender-Bares. (2020a). Linking leaf spectra to the plant tree of life. Pages 155-172 *in* J. Cavender-Bares, J. A. Gamon, and P. A. Townsend, editors. *Remote Sensing of Plant Biodiversity*. Springer.

Meireles, J. E., J. Cavender-Bares, P. A. Townsend, S. Ustin, J. A. Gamon, A. K. Schweiger, M. E. Schaepman, G. P. Asner, R. E. Martin, A. Singh, F. Schrodt, A. Chlus, and B. O'Meara. (2020b). Leaf reflectance spectra capture the evolutionary history of seed plants. *New Phytologist* 228:485-493.

Mevik, B.-H., Wehrens, R., & Liland, K. H. (2019). pls: Partial Least Squares and Principal Component Regression. R package version 2.7-1. https://CRAN.R-project.org/package=pls

Nakaji, T., Oguma, H., Nakamura, M., Kachina, P., Asanok, L., Marod, D., Aiba, M., Kurokawa, H., Kosugi, Y., Kassim, A. R., & Hiura, T. (2019). Estimation of six leaf traits of East Asian forest tree

species by leaf spectroscopy and partial least square regression. *Remote Sensing of Environment*, *233*, 111381.

Nunes, M. H., Davey, M. P., & Coomes, D. A. (2017). On the challenges of using field spectroscopy to measure the impact of soil type on leaf traits. *Biogeosciences*, *14*(13), 3371–3385.

Perez, T. M., Rodriguez, J., & Heberling, J. M. (2020). Herbarium-based measurements reliably estimate three functional traits. *American Journal of Botany*, *107*(10), 1457–1464.

Pérez-Harguindeguy, N., Díaz, S., Garnier, E., Lavorel, S., Poorter, H., Jaureguiberry, P., Bret-Harte, M. S., Cornwell, W. K., Craine, J. M., Gurvich, D. E., et al. (2013). New handbook for standardised measurement of plant functional traits worldwide. *Australian Journal of Botany*, *61*(3), 167–234.

Peterson, D. L., Aber, J. D., Matson, P. A., Card, D. H., Swanberg, N., Wessman, C., & Spanner, M. (1988). Remote sensing of forest canopy and leaf biochemical contents. *Remote Sensing of Environment*, *24*(1), 85–108.

Petibon, F., Czyż, E. A., Ghielmetti, G., Hueni, A., Kneubühler, M., Schaepman, M. E., & Schuman, M. C. (2021). Variation in reflectance spectroscopy of European beech leaves captures phenology and biological hierarchies despite measurement uncertainties. *Remote Sensing of Environment*, *264*, 112601.

Prata, E. M. B., Sass, C., Rodrigues, D. P., Domingos, F. M. C. B., Specht, C. D., Damasco, G., Ribas, C. C., Fine, P. V. A., & Vicentini, A. (2018). Towards integrative taxonomy in Neotropical botany: Disentangling the Pagamea guianensis species complex (Rubiaceae). *Botanical Journal of the Linnean Society*, *188*(2), 213–231.

R Core Team. (2020). R: A language and environment for statistical computing. R Foundation for Statistical Computing, Vienna, Austria. URL https://www.R-project.org/.

Richardson, A. D., Duigan, S. P., & Berlyn, G. P. (2002). An evaluation of noninvasive methods to estimate foliar chlorophyll content. *New Phytologist*, *153*(1), 185–194.

Richardson, A. D., Aubrecht, D. M., Basler, D., Hufkens, K., Muir, C. D., & Hanssen, L. (2021). Developmental changes in the reflectance spectra of temperate deciduous tree leaves and implications for thermal emissivity and leaf temperature. *New Phytologist*, *229*(2), 791–804.

Schweiger, A. K., Cavender-Bares, J., Townsend, P. A., Hobbie, S. E., Madritch, M. D., Wang, R., Tilman, D., & Gamon, J. A. (2018). Plant spectral diversity integrates functional and phylogenetic components of biodiversity and predicts ecosystem function. *Nature Ecology & Evolution*, *2*(6), 976–982.

Schweiger, A. K. (2020). Spectral Field Campaigns: Planning and Data Collection. Pages 385-423 *in* J. Cavender-Bares, J. A. Gamon, and P. A. Townsend, editors. *Remote Sensing of Plant Biodiversity*. Springer.

Serbin, S. P., Singh, A., McNeil, B. E., Kingdon, C. C., & Townsend, P. A. (2014). Spectroscopic determination of leaf morphological and biochemical traits for northern temperate and boreal tree species. *Ecological Applications*, *24*(7), 1651–1669.

Serbin, S. P. & Townsend, P. A. (2020). Scaling Functional Traits from Leaves to Canopies. Pages 43-82 *in* J. Cavender-Bares, J. A. Gamon, and P. A. Townsend, editors. *Remote Sensing of Plant Biodiversity*. Springer.

Serbin, S. P., Wu, J., Ely, K. S., Kruger, E. L., Townsend, P. A., Meng, R., Wolfe, B. T., Chlus, A., Wang, Z., & Rogers, A. (2019). From the Arctic to the tropics: Multibiome prediction of leaf mass per area using leaf reflectance. *New Phytologist*, *224*(4), 1557–1568.

Streher, A. S., Torres, R. da S., Morellato, L. P. C., & Silva, T. S. F. (2020). Accuracy and limitations for spectroscopic prediction of leaf traits in seasonally dry tropical environments. *Remote Sensing of Environment*, *244*, 111828.

Sun, Y., Wong, A. K. C., & Kamel, M. S. (2009). Classification of imbalanced data: A review. *International Journal of Pattern Recognition and Artificial Intelligence*, *23*(04), 687–719.

Thiers, B. 2021. The world's herbaria 2020: A summary report based on data from Index Herbariorum. Available at http://sweetgum.nybg.org/science/ih/

Turner, B. L., Hayes, P. E., & Laliberté, E. (2018). A climosequence of chronosequences in southwestern Australia. *European Journal of Soil Science*, *69*(1), 69–85.

Wang, Z., Chlus, A., Geygan, R., Ye, Z., Zheng, T., Singh, A., Couture, J. J., Cavender-Bares, J., Kruger, E. L., & Townsend, P. A. (2020). Foliar functional traits from imaging spectroscopy across biomes in eastern North America. *New Phytologist*, *228*(2), 494–511.

Wieczorek, J., Bloom, D., Guralnick, R., Blum, S., Döring, M., Giovanni, R., Robertson, T., & Vieglais, D. (2012). Darwin Core: An Evolving Community-Developed Biodiversity Data Standard. *PLOS ONE*, *7*(1), e29715.

Wold, S. (1994). PLS for multivariate linear modeling. In H. van de Waterbeemd, editor. Chemometric methods in molecular design, methods and principles in medicinal chemistry, Verlag-Chemie (Weinheim, Germany), 195–218.

Yan, Z., Guo, Z., Serbin, S. P., Song, G., Zhao, Y., Chen, Y., Wu, S., Wang, J., Wang, X., Li, J., Wang, B., Wu, Y., Su, Y., Wang, H., Rogers, A., Liu, L., & Wu, J. (2021). Spectroscopy outperforms leaf trait relationships for predicting photosynthetic capacity across different forest types. *New Phytologist*, *232*(1), 134–147.

Yang, X., Tang, J., Mustard, J. F., Wu, J., Zhao, K., Serbin, S., & Lee, J.-E. (2016). Seasonal variability of multiple leaf traits captured by leaf spectroscopy at two temperate deciduous forests. *Remote Sensing of Environment*, 179, 1–12.

Supplementary Materials

Sampling

For each sample, we collected a large group of sunlit leaves (>3 h estimated sun exposure per day) at about the same vertical position—for trees, the same branch or neighboring branches from the same individual. We avoided leaves with noticeable damage from herbivores or pathogens. We measured fresh-leaf spectra and fresh-leaf mass in the field, froze leaf disks for pigment analyses, and transported samples in a cooler to the lab. We then measured other whole-leaf traits and divided the remainder of the sample into two groups: (1) a portion to be pressed, and (2) a portion whose leaves were dried at 65 °C for three days, ground using a cyclone mill with 2 mm mesh, redried at 65 °C, and stored for chemical analyses. We measured pressed-leaf spectra on the former portion prior to mounting, and ground-leaf spectra and chemical traits on the latter. Although these are distinct subsets of leaves, we treat them as identical in their trait values since they are divided at random from the larger, relatively homogeneous bulk sample. A minimum of one representative pressed specimen of each species at each site and date is prepared as a specimen at the Marie-Victorin Herbarium in Montréal, Québec, Canada.

We classified species' growth forms following the Database of Vascular Plants of Canada (VASCAN; Desmet & Brouillet 2013). We classified *Agonis flexuosa* as a tree and manually disambiguated some species listed as adopting either shrub or three growth forms.

Spectral measurements

For the Beauchamp-Rioux, Boucherville, and Warren projects, we measured fresh-leaf directional-hemispherical reflectance spectra on each sample in 2018 using an HR-1024i spectroradiometer outfitted with a DC-R/T integrating sphere from Spectra Vista Corporation (SVC; Poughkeepsie, NY, USA). We measured spectra on the adaxial surface of six leaves or, for small or narrow leaves, single-layer leaf arrays following the protocol in Noda et al. (2013) as adapted for our instrument (Laliberté & Soffer

2018a; Laliberté and Soffer 2018b). For the Dessain project, we measured fresh-leaf reflectance spectra in 2017 using a FieldSpec 4 spectroradiometer equipped with an RTS-3ZC integrating sphere from Analytical Spectral Devices, Inc. (ASD; Boulder, CO, USA) following the leaf spectroscopy protocol from the Global Airborne Observatory (https://gao.asu.edu/spectranomics-protocols). We collected spectra from a variable number of leaves or arrays per sample—six in most cases, but as few as three or as many as eighteen from certain samples. For all projects, each reflectance measurement was calibrated against a white Spectralon 99% reflectance panel and corrected for stray light.

For all projects, we measured reflectance spectra on the adaxial surface of pressed, intact leaf samples using a PSR+ 3500 spectroradiometer with a leaf clip foreoptic (Spectral Evolution, Haverhill, MA) between six months and three years after collection. We calibrated reflectance against a white Spectralon reflectance panel and measured 3-7 spectra per sample. Although all samples were pressed in a plant press, some nevertheless dried in a way that created an uneven leaf surface. We noted any visible discoloration that samples underwent during drying or storage, including browning or blackening. In general, we aimed to avoid uneven or discolored areas when measuring spectra, although it was sometimes not entirely possible when discoloration was pervasive.

For all projects, we also measured ground-leaf spectra using the PSR+ 3500 spectroradiometer with a benchtop reflectance probe foreoptic that pressed loose powder into a smooth, even pellet. For each sample, we added at least 0.6 g of leaf powder into a sample tray; in preliminary tests, adding additional material did not change the spectra, suggesting that transmittance was close to zero. We calibrated reflectance against a white Spectralon reflectance panel placed in an identical sample tray. We measured three spectra per sample on the same pellet, turning the sample tray 120° between the first two spectra, and loosening and mixing the powder before reshaping the pellet between the second and third spectra.

A small number of specimens did not have usable spectra at all three stages, usually either due to lack of enough pressed or ground material or to poor spectral quality at any stage. To ensure fair comparisons among the stages, we removed any sample from the dataset that was not available for at least two stages. Among the remaining samples, any sample that was not available for all three stages (<4%) was placed in the training subset for PLSR analyses.

Our spectral processing pipeline varied by the type of data. Although the actual spectral resolution was more variable and coarser, the ASD Field Spec 4 and Spectral Evolution PSR+ 3500 spectrometers' software automatically resampled the spectra to 1 nm resolution and interpolated over the overlap region between sensors (Schweiger & Laliberté 2020). For data from the SVC HR-1024i spectrometer, we performed these steps using linear interpolation. For pressed-leaf spectra only, we detected jumps in reflectance at the sensor overlap region and removed them using the function *match_sensors()* in *R* package *spectrolab v. 0.0.10* (Meireles et al. 2017). Next, we averaged all spectra for a given sample and tissue type (fresh, pressed, or ground). Spectra measured with integrating spheres tend to have greater noise, especially at the ends. To reduce noise in fresh-leaf spectra, we applied a Savitzky-Golay filter using *R* package *signal 0.7.6* (Signal Developers, 2013), with varying order and length: order 3 and length 21 from 350-715 nm, order 3 and length 35 from 715-1390 nm, order 3 and length 75 from 1390-1880 nm, and order 5 and length 175 from 1880-2500 nm. Finally, we trimmed all spectra to 400-2400 nm, removing the extremes where sensors show greater noise. We did all spectral processing in *R v. 3.6.3* (R Core Team 2020) using *spectrolab v. 0.0.10* (Meireles et al. 2017).

Leaf trait measurements

We performed all leaf trait measurements excluding petioles, but including the rachis for compound leaves, since the rachis is functionally analogous to the midrib of a simple leaf. We measured the following leaf structural and chemical traits: Leaf mass per area (LMA; kg m^{-2}), leaf dry matter content (LDMC; mg g^{-1}), equivalent water thickness (EWT; cm), carbon fractions (soluble cell contents,

hemicellulose, cellulose, and lignin) on a mass basis, pigments (chlorophyll *a*, chlorophyll *b*, and total carotenoids) on a mass basis, and concentrations of a variety of elements (Al, C, Ca, Cu, Fe, K, Mg, Mn, N, Na, P, Zn).

From a subset of the leaves for each sample whose fresh-leaf spectra we measured, we used a 7 mm cork borer to punch leaf disks (or cut fragments of narrow leaves) in the field and stored them on ice in the darkness before transferring them to a -80 °C freezer in the lab. We extracted pigments under darkness in an $MgCO_3$-MeOH solution and estimated pigment concentrations using a spectrophotometric protocol on a SPECTROstar Nano microplate reader (BMG LABTECH, Ortenburg, Germany; Girard et al. 2020).

From a separate subset of leaves from each sample, we weighed fresh mass in the field shortly after collection. We then rehydrated the leaves in sealed plastic bags with damp paper towels for at least 12 h and weighed them for rehydrated mass. We scanned leaves and estimated their area using WinFOLIA (Regent Instruments, Québec, QC, CA). Lastly, we dried them for at least 72 h in a drying oven at 65°C before reweighing for dry mass. We calculated LDMC as total dry mass divided by total fresh mass and LMA as total dry mass divided by total rehydrated area (Laliberté 2018). We further calculated EWT from LDMC and LMA.

We analyzed ground bulk tissue samples for N and C using a Vario MICRO Cube combustion analyzer (Elementar, Langenselbold, Germany; Ayotte et al. 2019). We analyzed the same samples for other elements (Al, Ca, Cu, Fe, K, Mg, Mn, Na, P, Zn) using inductively coupled plasma-mass spectrometry (ICP-MS; **citation to protocol; equipment details**). We removed five data points from the ICP-MS output as extreme outliers that were not representative of the range of concentrations of their respective elements across our samples. We also set values below the detection limit, which sometimes returned as negative concentrations, to zero.

Finally, we analyzed the samples for carbon fractions using an ANKOM 2000 Fiber Analyzer (Ankom Technology, Macedon, New York, USA) to perform a sequence of digestions (Ayotte & Laliberté 2019). The first digestion in a heated neutral detergent washes off soluble cell contents. The second digestion in a heated acidic detergent removes hemicellulose and bound proteins—which, for simplicity, we just refer to as hemicellulose. The third digestion in 70% sulfuric acid removes cellulose, leaving behind lignin and recalcitrant compounds. We used the change in each bag's mass between stages to determine the mass of each fraction. We ashed all samples and used ash content as a correction factor to calculate the ash-free lignin fraction.

External validation dataset

From August to November 2018, we collected 333 samples for an external validation dataset at Cedar Creek Ecosystem Science Reserve (East Bethel, MN, USA). These samples included broadleaf trees (n = 177; 10 species), coniferous needleleaf trees (n = 101; 4 species), and herbs (n = 55; 14 species). Most samples were from the Forests and Biodiversity (FAB) experiment (Grossman et al. 2017), the Biodiversity in Willows and Poplars (BiWaP) experiment (Grossman & Cavender-Bares 2019), and the Big Biodiversity (BioDIV or e120) experiment (Tilman et al. 1997), although some were from other parts of the site.

Each sample included multiple leaves from the same individual, taken when possible from a nearby position on the plant. Unlike in the CABO dataset, we collected samples from any part of an individual, not just sunlit leaves. From each sample, we designated one leaf for fresh mass to be measured immediately following collection; this leaf ('fresh-mass subsample') was stored separately and its spectra were labeled to keep track of its identity. (For conifers or other plants with small or narrow leaves, we often included multiple leaves in this fresh mass sample.) We took and flash-froze 3-5 hole punches from another leaf (or group of leaves) for pigment analyses ('pigment subsample'; pigment data not shown);

this leaf and its spectra were also labeled separately. We collected more leaves to have enough tissue for a bulk chemical sample, but did not keep track of them individually.

In the field, we measured multiple fresh-leaf spectra per sample (not shown here) using a PSR+ 3500 spectroradiometer with a leaf clip foreoptic (Spectral Evolution, Haverhill, MA) and placed the leaves in sealed plastic bags with a damp paper towel. These bags were kept in coolers until the end of the sampling day. We weighed the fresh-mass subsample immediately upon return to the lab and kept all leaves in a refrigerator until we scanned the fresh-mass and pigment subsamples within the next few days. After scanning, we placed all leaves in flat paper bags and pressed them for 2-3 hours in a plant press before removing them and placing them in a drying shed at 40 °C for at least one week. This deviates from most standard herbarium protocols, including the one used in the CABO project, where leaves are kept in the press while drying and subjected to a higher temperature for a shorter time. After we dried the leaves, we weighed the fresh-mass and pigment subsamples. Certain species, especially *Populus tremuloides*, seemed especially prone to discoloration during sample preparation.

In May 2020, we measured pressed-leaf spectra using a PSR+ 3500 spectroradiometer with a leaf clip foreoptic. We did not use a specific protocol for small or narrow leaves, but aimed to arrange leaves in a way that minimized overlaps or gaps. We removed spectra with especially low (<40%) or high (>80%) peak reflectance, and any with major visible gaps in the sensor overlap regions. We measured three spectra per subsample except in cases where getting high-quality spectra proved especially difficult. We then removed the petioles (when applicable) and put leaves in scintillation vials with ball bearings to grind the tissue in a paint shaker, combining all subsamples from a given sample. We then dried samples again and measured C and N with an elemental analyzer (Costech ECS 4010 Analyzer, Valencia, California, USA).

For estimating LMA, LDMC, and EWT, we only used the spectra from the fresh-mass subsample. For C and N, we used all spectra from a given sample, ignoring the subsample labels. As among the CABO pressed-leaf spectra, we first matched sensors, then averaged spectra within the relevant sample or subsample, and lastly trimmed them to 400-2400 nm.

We applied the ensemble of models resulting from our 100× jackknife analysis on the pressed-leaf CABO data and applied them to the Cedar Creek data. We also applied the model ensemble from the pressed-leaf CABO data restricted to 1300-2400 nm to the Cedar Creek data restricted to the same range. We calculated summary statistics and plotted results as in the internal validation.

Supplementary references

Ayotte, J., Guilbeault-Mayers, X., & Laliberté, E. (2019). Measuring CN content in leaf samples using Elementar Vario MICRO Cube. https://doi.org/10.17504/protocols.io.udces2w

Ayotte, J., & Laliberté, E. (2019). Measuring leaf carbon fractions with the ANKOM2000 Fiber Analyzer. https://doi.org/10.17504/protocols.io.yinfude

Desmet, P., & Brouillet, L. (2013). Database of Vascular Plants of Canada (VASCAN): A community contributed taxonomic checklist of all vascular plants of Canada, Saint Pierre and Miquelon, and Greenland. *PhytoKeys*, *25*, 55–67.

Girard, A., Ayotte, J., & Laliberté, E. (2020). Measuring chlorophylls and carotenoids in plant tissue. **(insert DOI once published)**

Grossman, J. J., & Cavender-Bares, J. (2019). Consequences of biodiversity shift across phylogenetic scales for aspen and willow growth, survival, and herbivory. *Journal of Vegetation Science*, *30*(2), 301–311.

Grossman, J. J., Cavender-Bares, J., Hobbie, S. E., Reich, P. B., & Montgomery, R. A. (2017). Species richness and traits predict overyielding in stem growth in an early-successional tree diversity experiment. *Ecology*, *98*(10), 2601–2614.

Laliberté, E. (2018). Measuring specific leaf area and water content. https://doi.org/10.17504/protocols.io.p3tdqnn

Laliberté, E., & Soffer, R. (2018a). Measuring spectral reflectance and transmittance (350-2500 nm) of large leaves using the Spectra Vista Corporation (SVC) DC-R/T Integrating Sphere. https://doi.org/10.17504/protocols.io.p8pdrvn

Laliberté, E., & Soffer, R. (2018b). Measuring spectral reflectance and transmittance (350-2500 nm) of small and/or narrow leaves using the Spectra Vista Corporation (SVC) DC-R/T Integrating Sphere. https://doi.org/10.17504/protocols.io.q56dy9e

Meireles, J., Schweiger, A., & Cavender-Bares, J. (2017). spectrolab: Class and Methods for Hyperspectral Data in R. R package version 0.0.10. https://CRAN.R-project.org/package=spectrolab

Noda, H. M., Motohka, T., Murakami, K., Muraoka, H., & Nasahara, K. N. (2013). Accurate measurement of optical properties of narrow leaves and conifer needles with a typical integrating sphere and spectroradiometer. *Plant, Cell & Environment*, *36*(10), 1903–1909.

R Core Team. (2020). R: A language and environment for statistical computing. R Foundation for Statistical Computing, Vienna, Austria. URL https://www.R-project.org/.

Schweiger, A. K., & Laliberté, E. (2020). Processing of leaf spectra. https://doi.org/10.17504/protocols.io.bhsdj6a6

Signal Developers (2013). signal: Signal processing. http://r-forge.r-project.org/projects/signal/.

Tilman, D., Knops, J., Wedin, D., Reich, P., Ritchie, M., & Siemann, E. (1997). The Influence of Functional Diversity and Composition on Ecosystem Processes. *Science*, *277*(5330), 1300–1302.

Supplementary tables

Table S1: Summary statistics of PLSR model internal validation from pressed-leaf spectra restricted to 1300-2500 nm. %RMSE is calculated as RMSE divided by the 2.5% trimmed range of data within either the training data set (calibration) or the testing data set (validation).

Trait	No. comps	R^2	RMSE	%RMSE
LMA (kg m^{-2})	7	0.902	0.0125	7.94
LDMC (mg g^{-1})	10	0.694	37.6	12.8
EWT (cm)	10	0.767	0.00222	13.3
Solubles (%)	10	0.712	4.25	13.5
Hemicellulose (%)	10	0.733	2.48	15.6
Cellulose (%)	11	0.745	1.50	17.9
Lignin (%)	11	0.638	2.07	16.7
C (%)	11	0.811	0.987	10.8
N (%)	9	0.772	0.273	11.5
Chl *a* (mg g^{-1})	7	0.582	1.37	17.3
Chl *b* (mg g^{-1})	7	0.514	0.506	18.7
Carotenoids (mg g^{-1})	7	0.599	0.280	17.9
Al (mg g^{-1})	6	0.210	0.0420	24.7
Ca (mg g^{-1})	11	0.723	3.72	13.2
Cu (mg g^{-1})	8	0.243	0.00676	24.0
Fe (mg g^{-1})	4	0.223	0.0391	20.9
K (mg g^{-1})	11	0.566	2.93	18.6
Mg (mg g^{-1})	11	0.413	0.733	20.1
Mn (mg g^{-1})	10	0.368	0.140	22.4
Na (mg g^{-1})	12	0.434	0.577	20.6
P (mg g^{-1})	11	0.507	0.772	19.0
Zn (mg g^{-1})	9	0.295	0.0712	25.1

Table S2: Summary statistics for external validation of pressed-leaf PLSR models, restricting the range of spectra to 1300-2500 nm. The models were trained on CABO data (see Table S1) and applied to a dataset collected at Cedar Creek.

	Including conifers			Excluding conifers		
Trait	R^2	RMSE	%RMSE	R^2	RMSE	%RMSE
LMA (kg m^{-2})	0.867	0.0195	10.8	0.746	0.0111	13.7
LDMC (mg g^{-1})	0.468	51.2	18.1	0.461	53.4	18.5
EWT (cm)	0.608	0.00512	20.7	0.633	0.00318	17.6
C (%)	0.007	4.54	26.0	0.023	4.38	28.2
N (%)	0.622	0.666	34.7	0.614	0.772	30.3

Supplementary figures

Fig. S1: Two researchers (A. Scott and I. Clark) demonstrate a typical setup for measuring pressed-leaf spectra with a PSR+ 3500 spectroradiometer and leaf clip on unmounted pressed specimens. The specimen shown here was not part of this study. (Photo: Jeannine Cavender-Bares)

Fig. S2: Internal validation results for predictions of LMA, LDMC, and EWT from fresh- (left), pressed- (middle), and ground-leaf (right) spectra. In each panel, each functional group has a separate ordinary least-squares regression line overlaid on top of the thick dashed 1:1 line. The error bars for each data point are 95% confidence intervals calculated from the distribution of predictions based on the ensemble of 100 models produced from jackknife analyses.

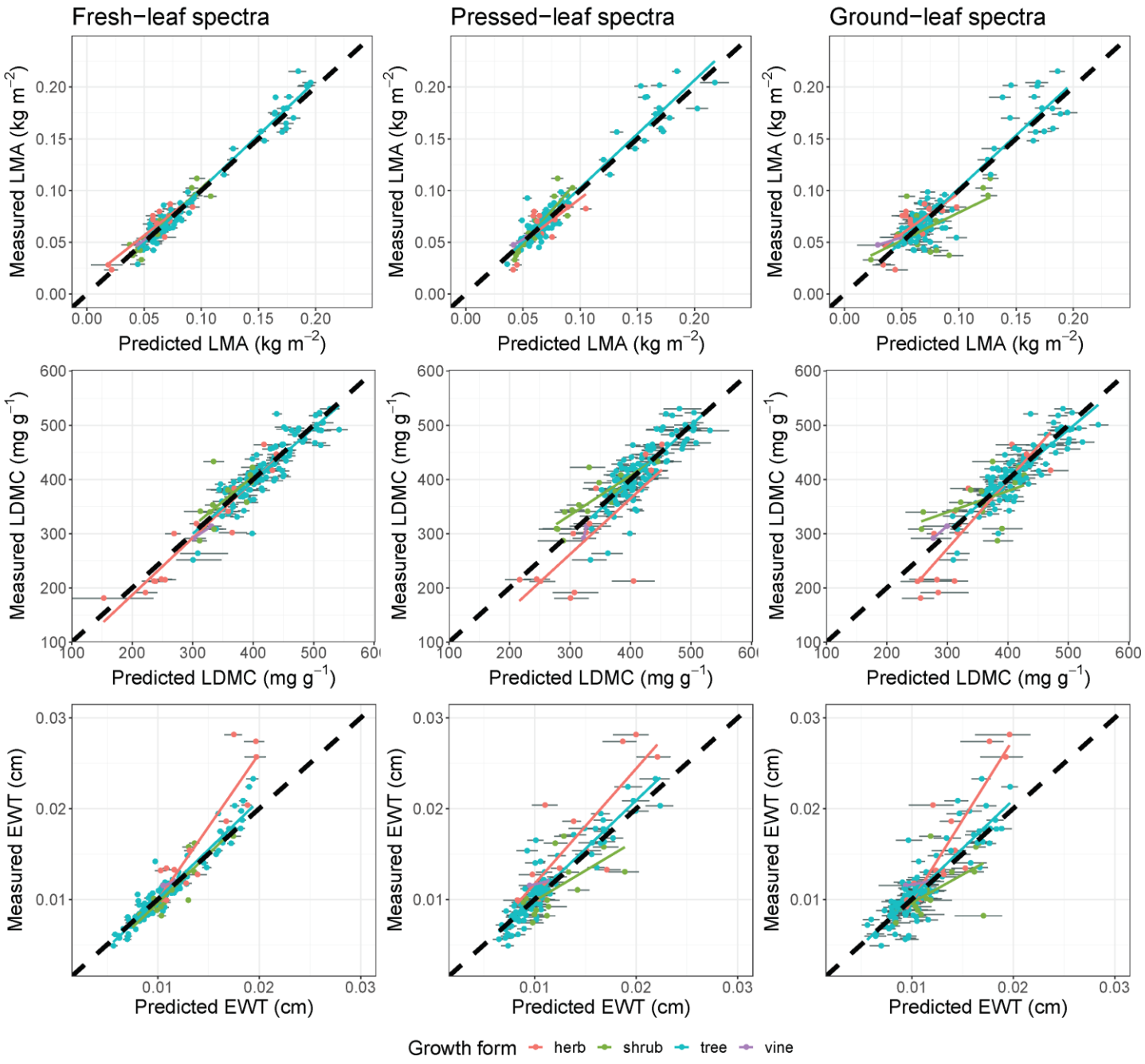

Fig. S3: Internal validation results for predictions of C, N, and P from fresh- (left), pressed- (middle), and ground-leaf (right) spectra, displayed as in Fig. S2.

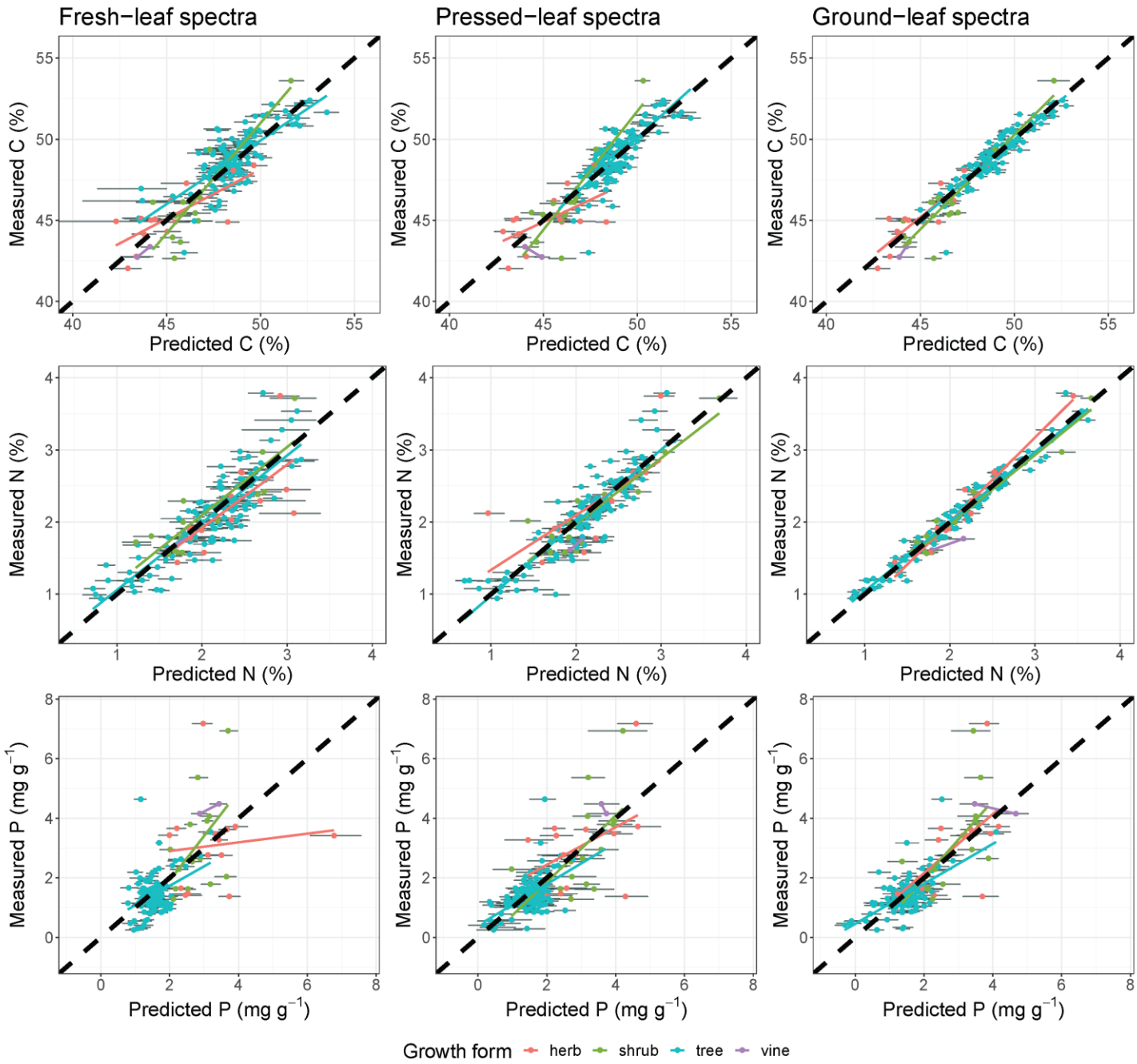

Fig. S4: Internal validation results for predictions of soluble cell contents, hemicellulose, cellulose, and lignin from fresh- (left), pressed- (middle), and ground-leaf (right) spectra, displayed as in Fig. S2.

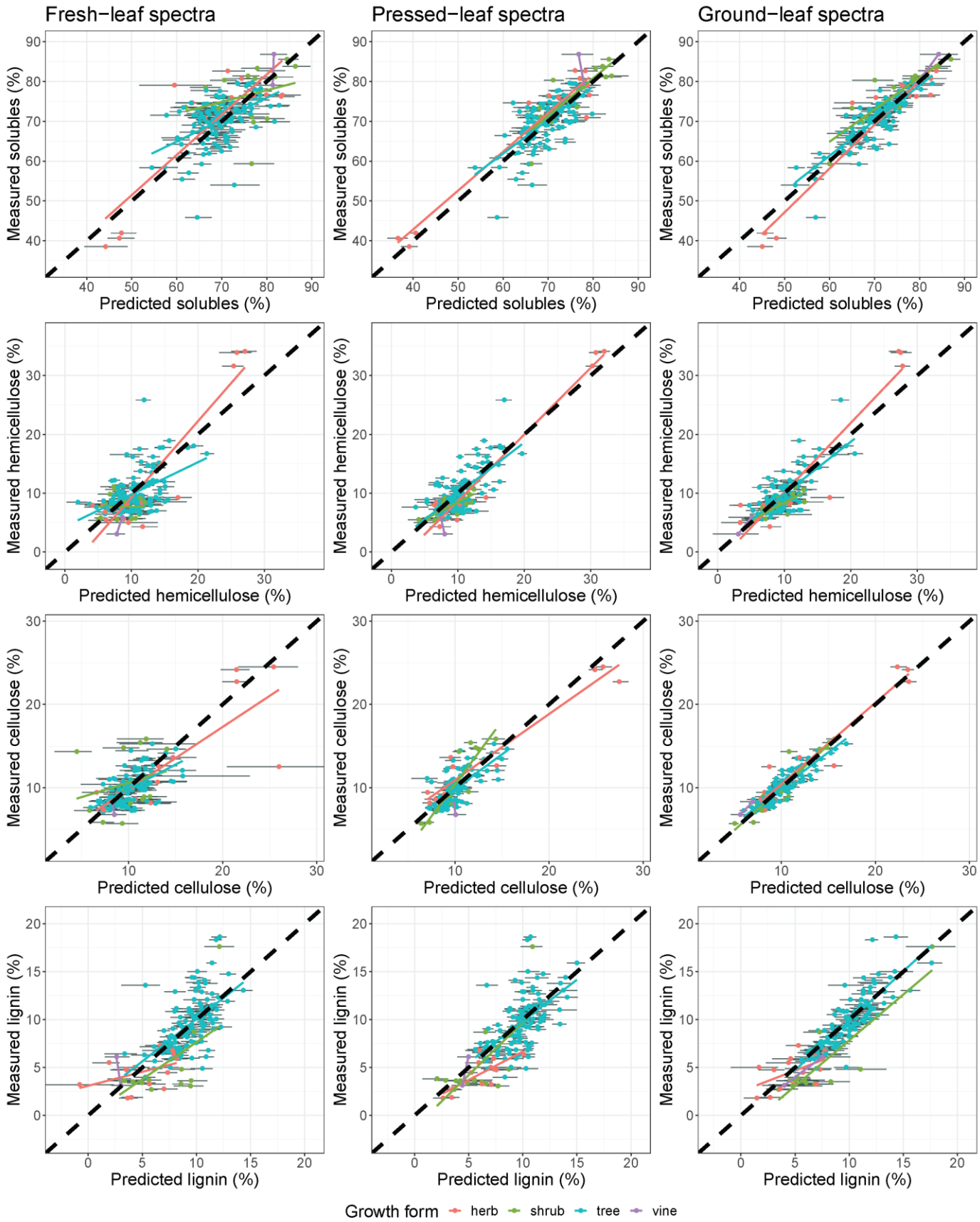

Fig. S5: Internal validation results for predictions of chlorophyll *a*, chlorophyll *b*, and total carotenoids from fresh- (left), pressed- (middle), and ground-leaf (right) spectra, displayed as in Fig. S2.

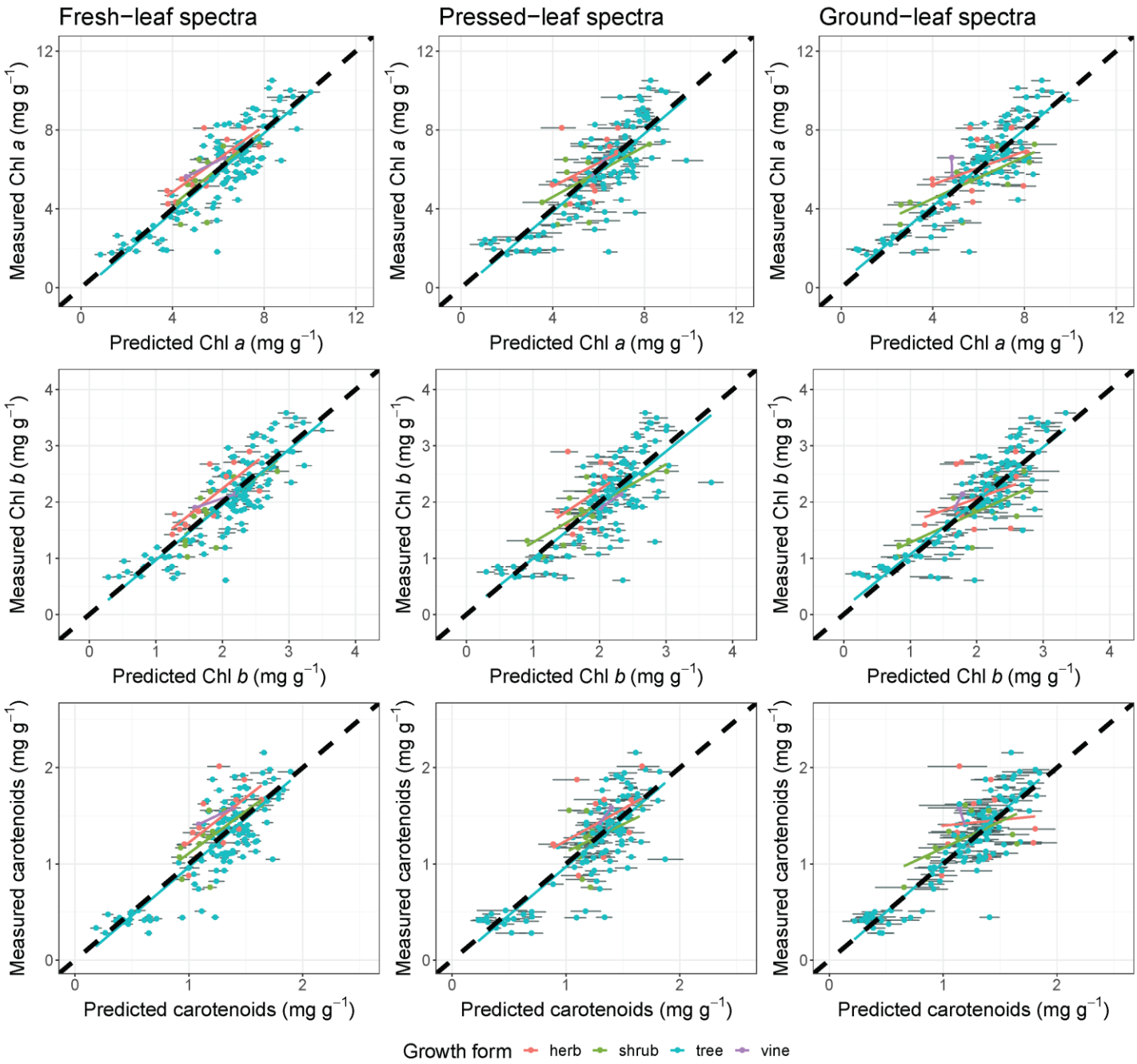

Fig. S6: Internal validation results for predictions of Al, Ca, and Cu from fresh- (left), pressed- (middle), and ground-leaf (right) spectra, displayed as in Fig. S2.

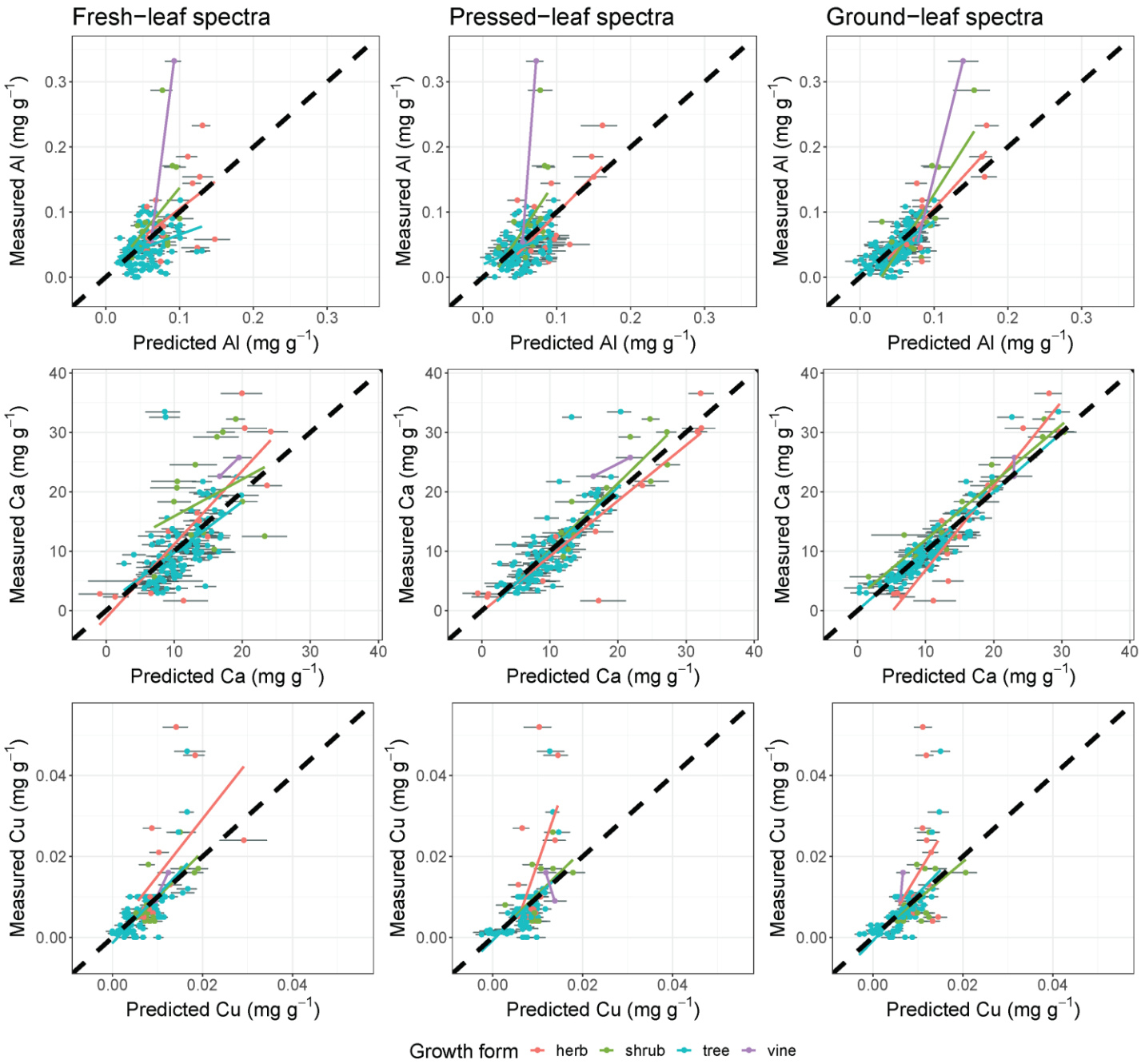

Fig. S7: Internal validation results for predictions of Fe, K, and Mg from fresh- (left), pressed- (middle), and ground-leaf (right) spectra, displayed as in Fig. S2.

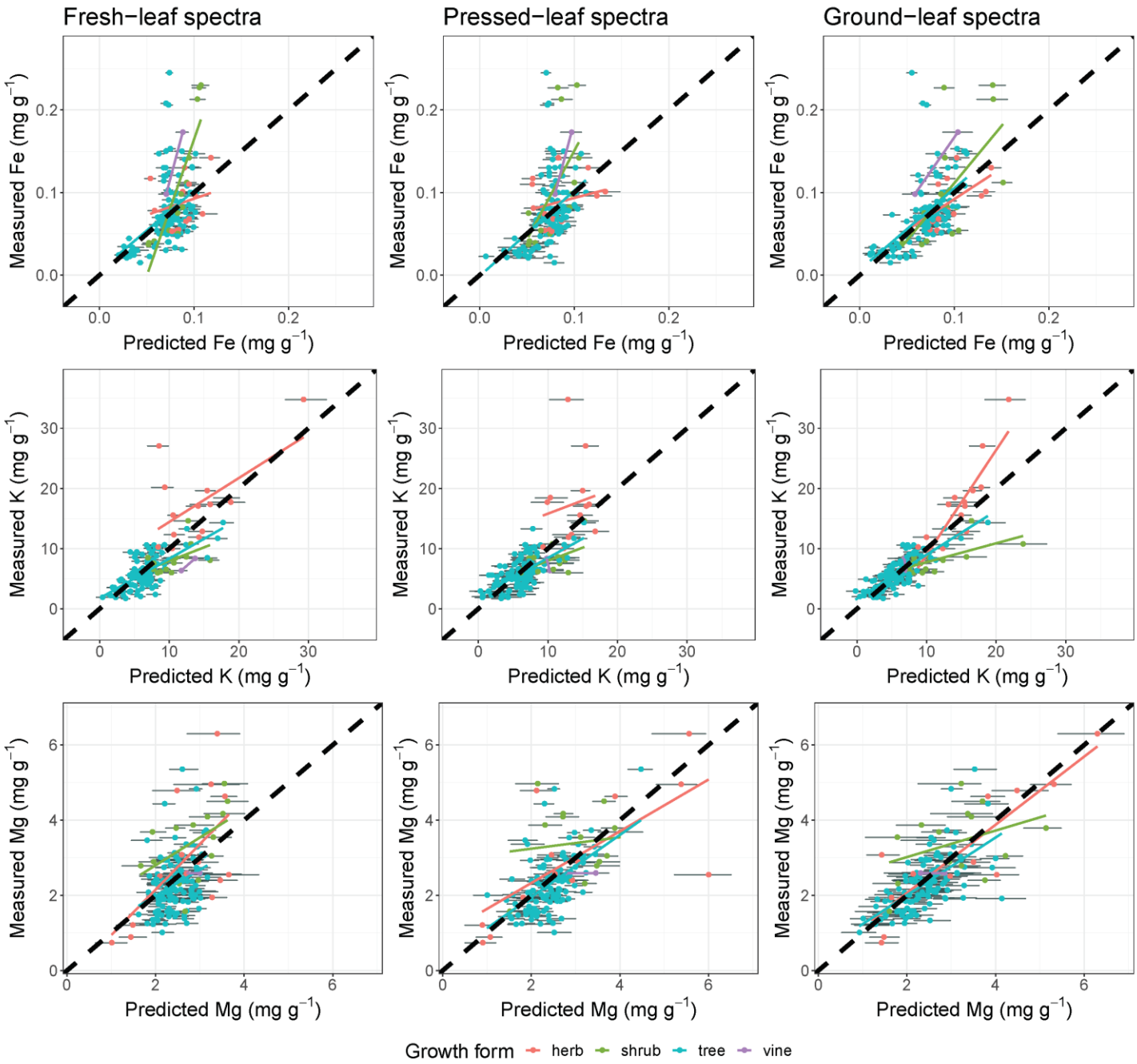

Fig. S8: Internal validation results for predictions of Mn, Na, and Zn from fresh- (left), pressed- (middle), and ground-leaf (right) spectra, displayed as in Fig. S2.

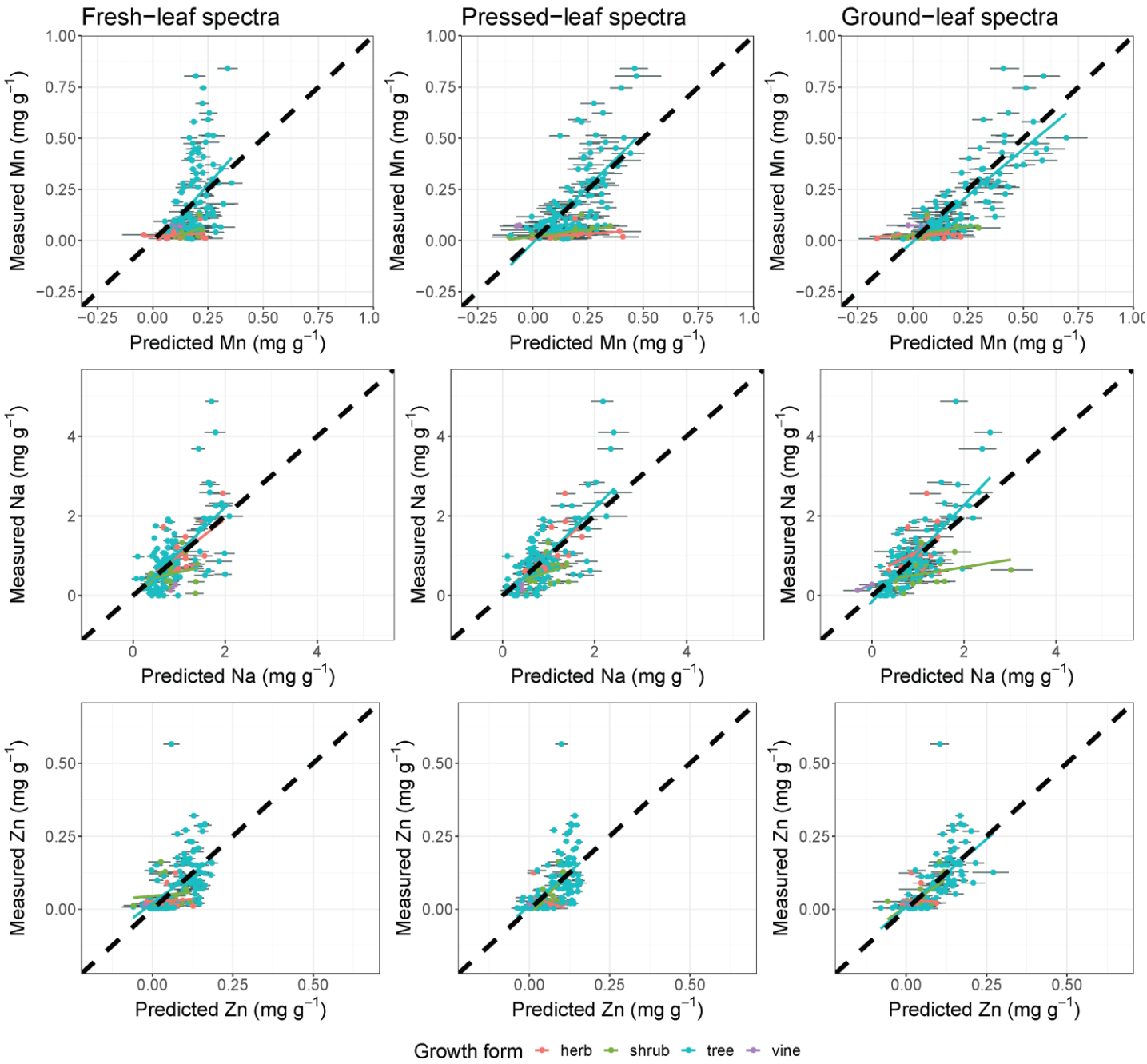

Fig. S9: The distributions of fresh-leaf spectral model performance statistics for each trait based on 100 jackknife resamples from the calibration data set. The red dots show the R^2 and %RMSE from applying the ensemble of models to the internal validation subset. Abbreviations: sol = solubles, hemi = hemicellulose, cell = cellulose, lign = lignin, car = total carotenoids.

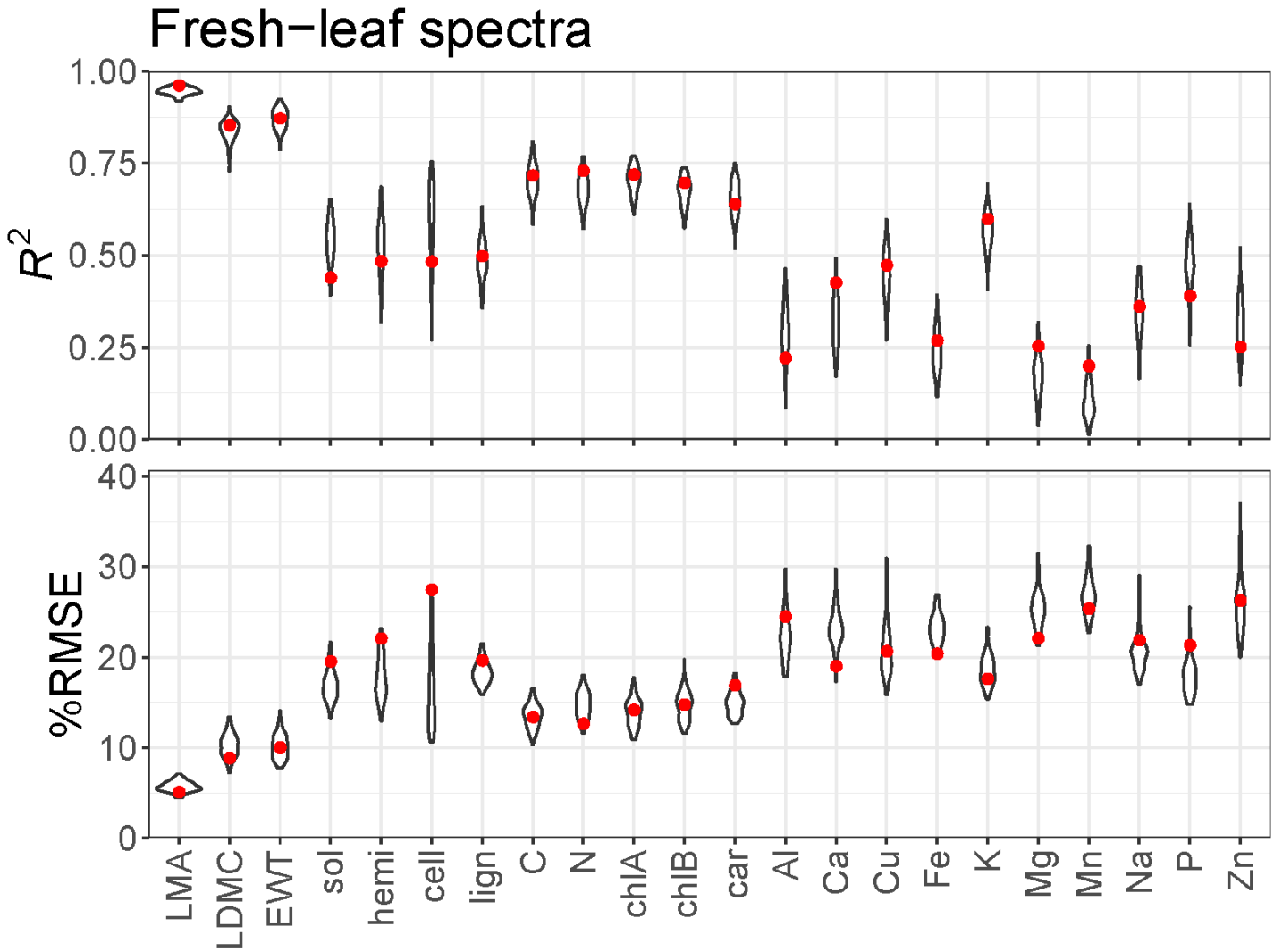

Fig. S10: The distributions of pressed-leaf spectral model performance statistics for each trait based on 100 jackknife resamples from the calibration data set. The red dots show the R^2 and %RMSE from applying the ensemble of models to the internal validation subset. Abbreviations: sol = solubles, hemi = hemicellulose, cell = cellulose, lign = lignin, car = total carotenoids.

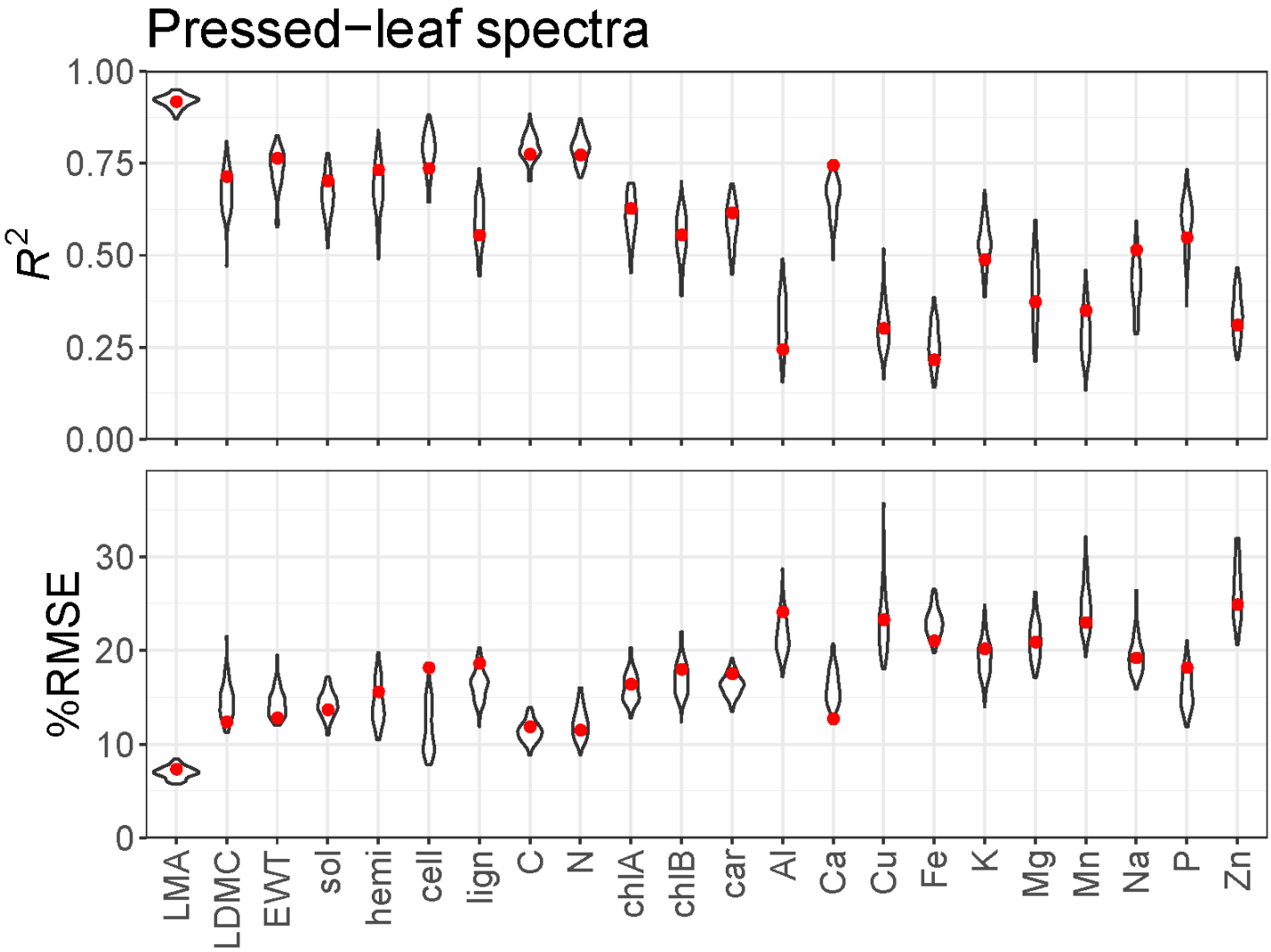

Fig. S11: The distributions of ground-leaf spectral model performance statistics for each trait based on 100 jackknife resamples from the calibration data set. The red dots show the R^2 and %RMSE from applying the ensemble of models to the internal validation subset. Abbreviations: sol = solubles, hemi = hemicellulose, cell = cellulose, lign = lignin, car = total carotenoids.

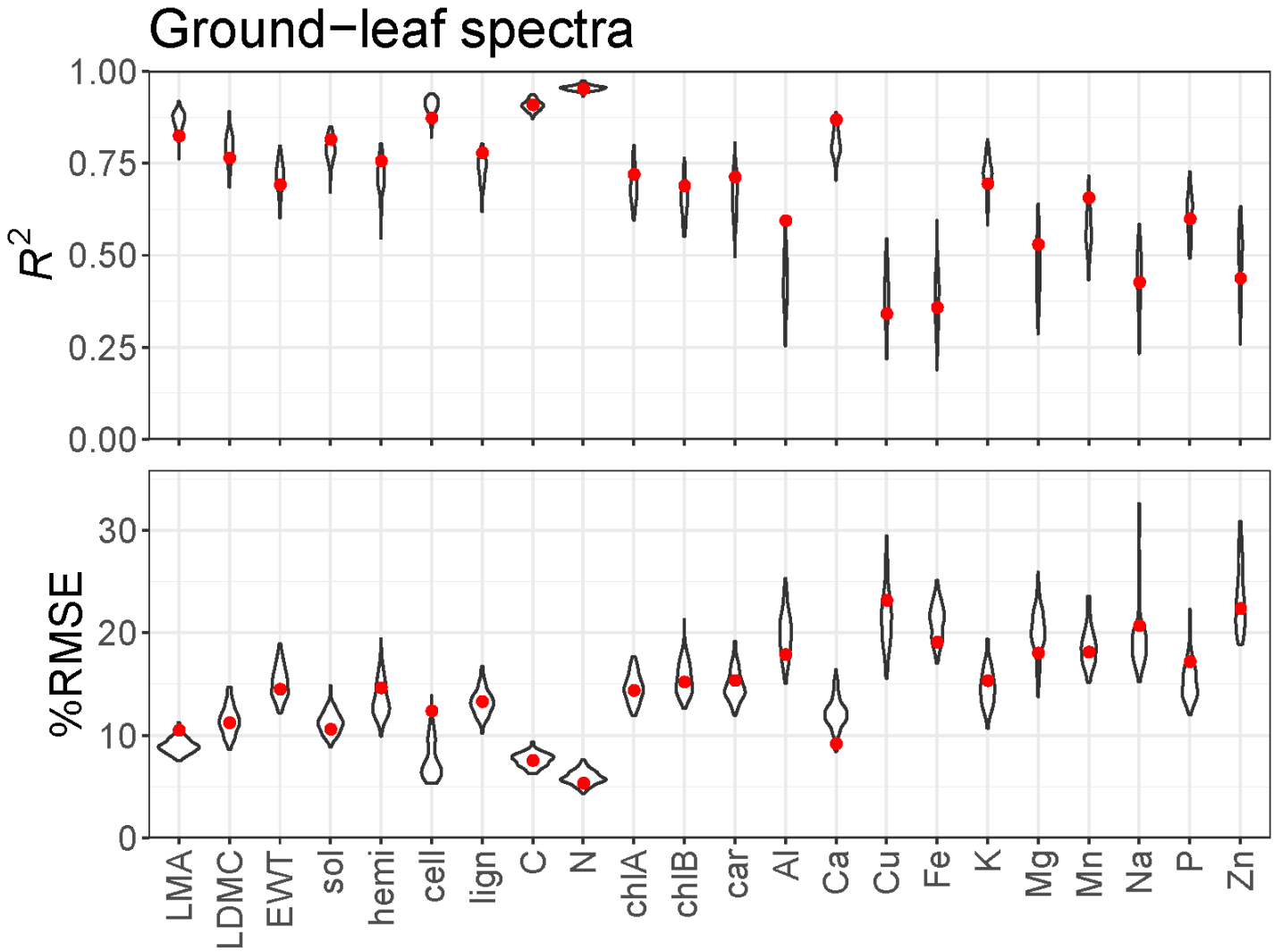

Fig. S12: The variable importance of projection (VIP) metric calculated for all traits from fresh-leaf spectra. Abbreviations: sol = solubles, hemi = hemicellulose, cell = cellulose, lign = lignin, car = total carotenoids. The dashed horizontal line at 0.8 represents a heuristic threshold for importance suggested by Burnett et al. (2021).

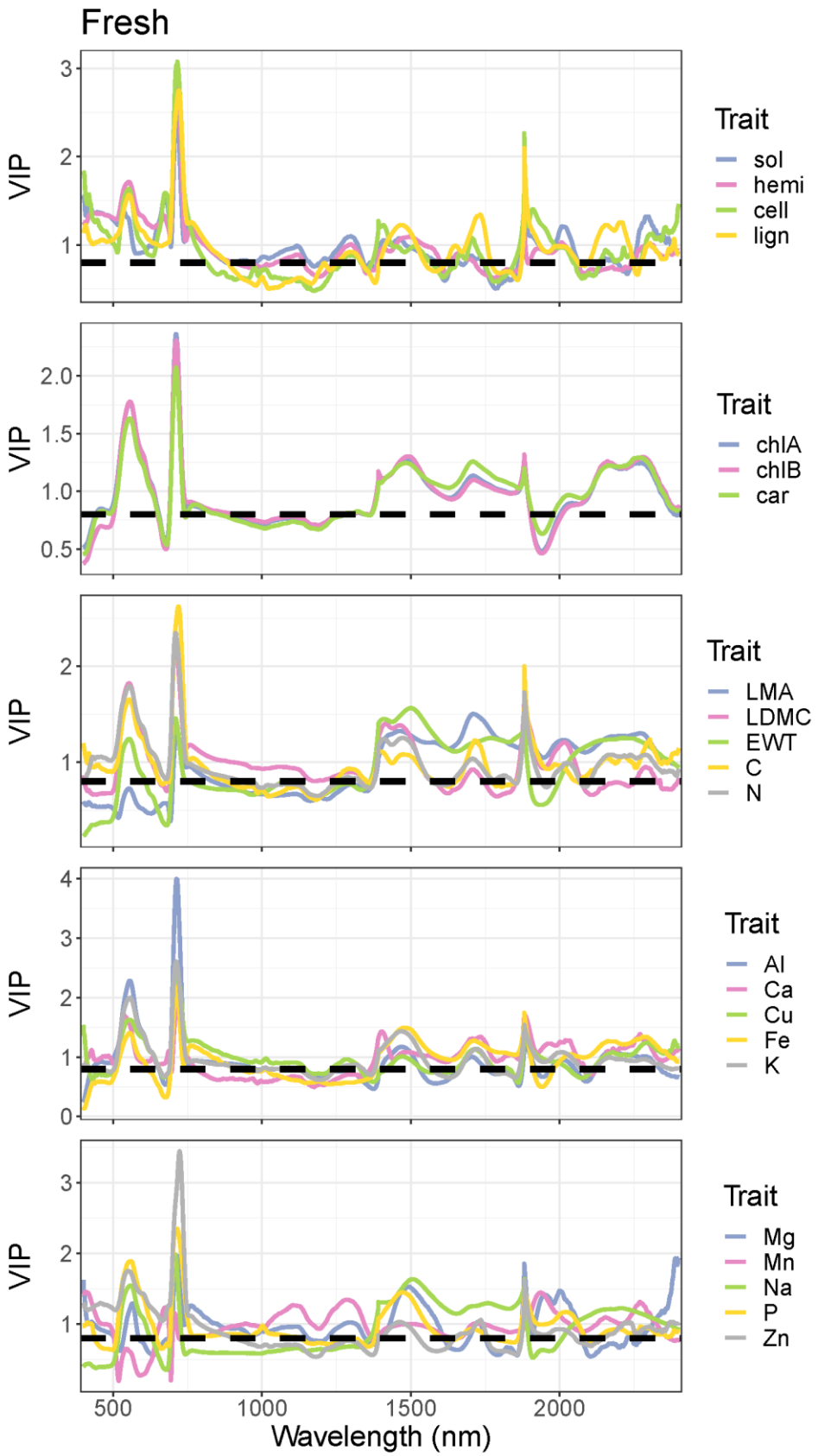

Fig. S13: The variable importance of projection (VIP) metric calculated for all traits from pressed-leaf spectra. Abbreviations: sol = solubles, hemi = hemicellulose, cell = cellulose, lign = lignin, car = total carotenoids. The dashed horizontal line at 0.8 represents a heuristic threshold for importance suggested by Burnett et al. (2021).

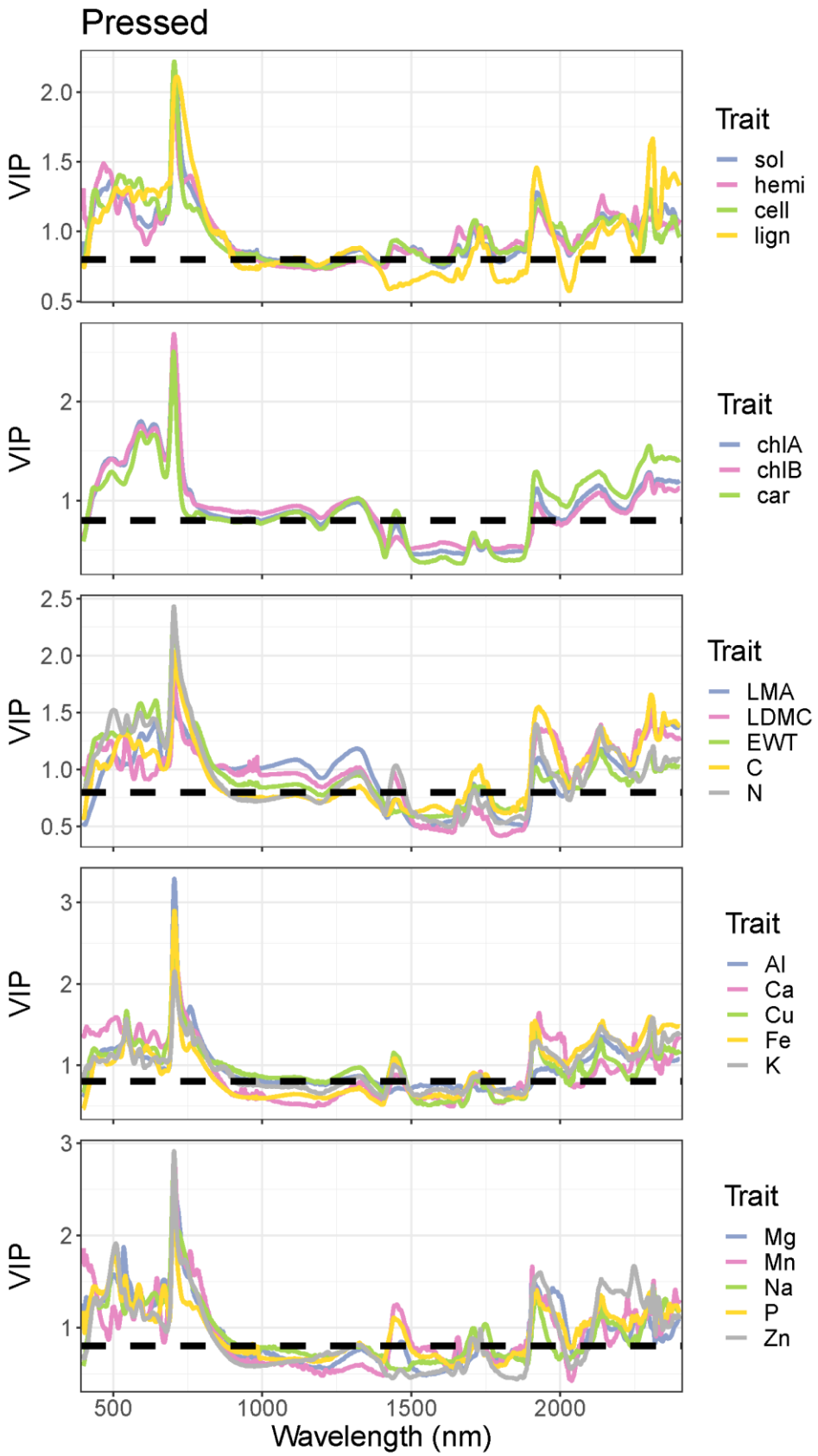

Fig. S14: The variable importance of projection (VIP) metric calculated for all traits from ground-leaf spectra. Abbreviations: sol = solubles, hemi = hemicellulose, cell = cellulose, lign = lignin, car = total carotenoids. The dashed horizontal line at 0.8 represents a heuristic threshold for importance suggested by Burnett et al. (2021).

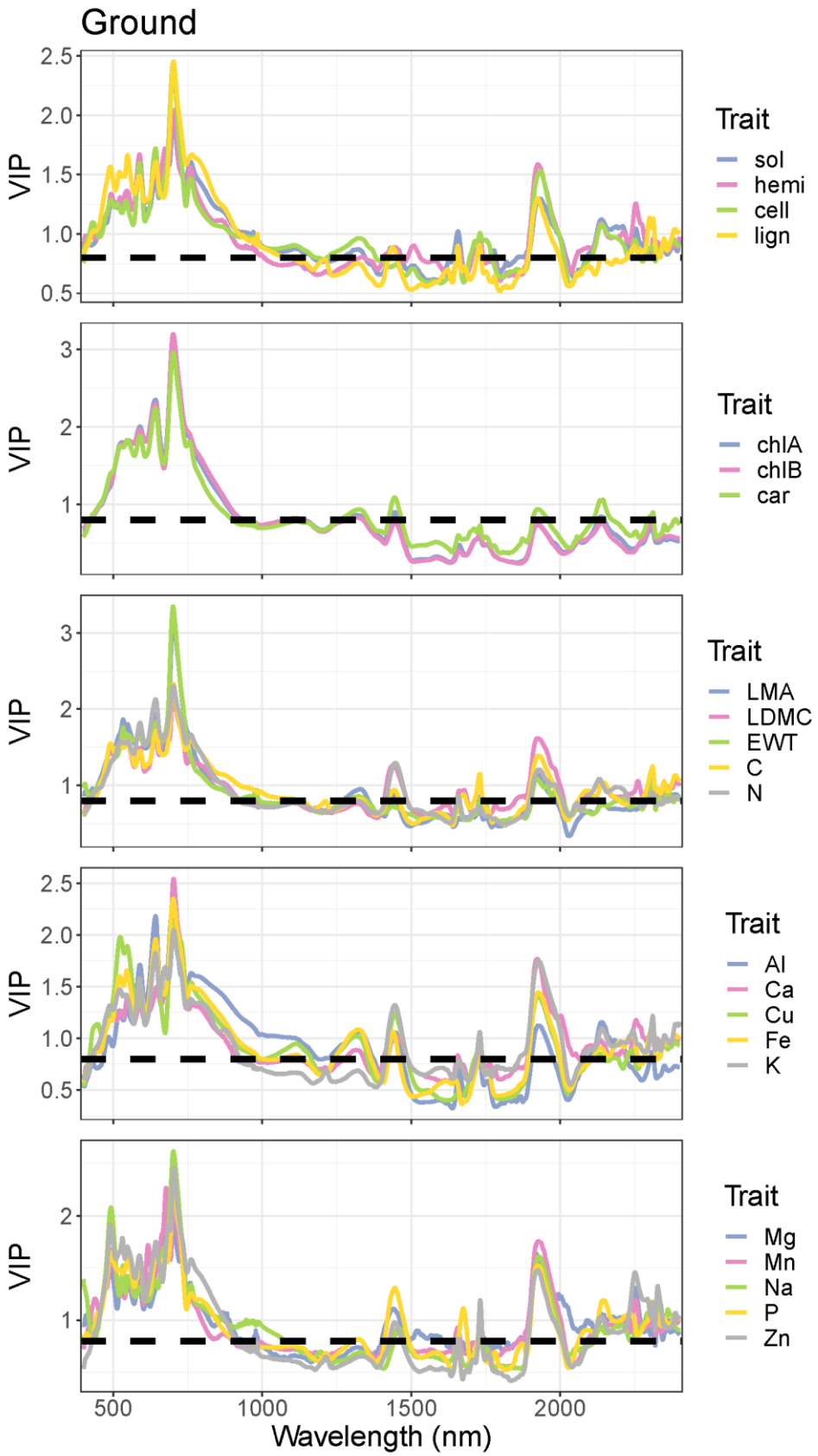
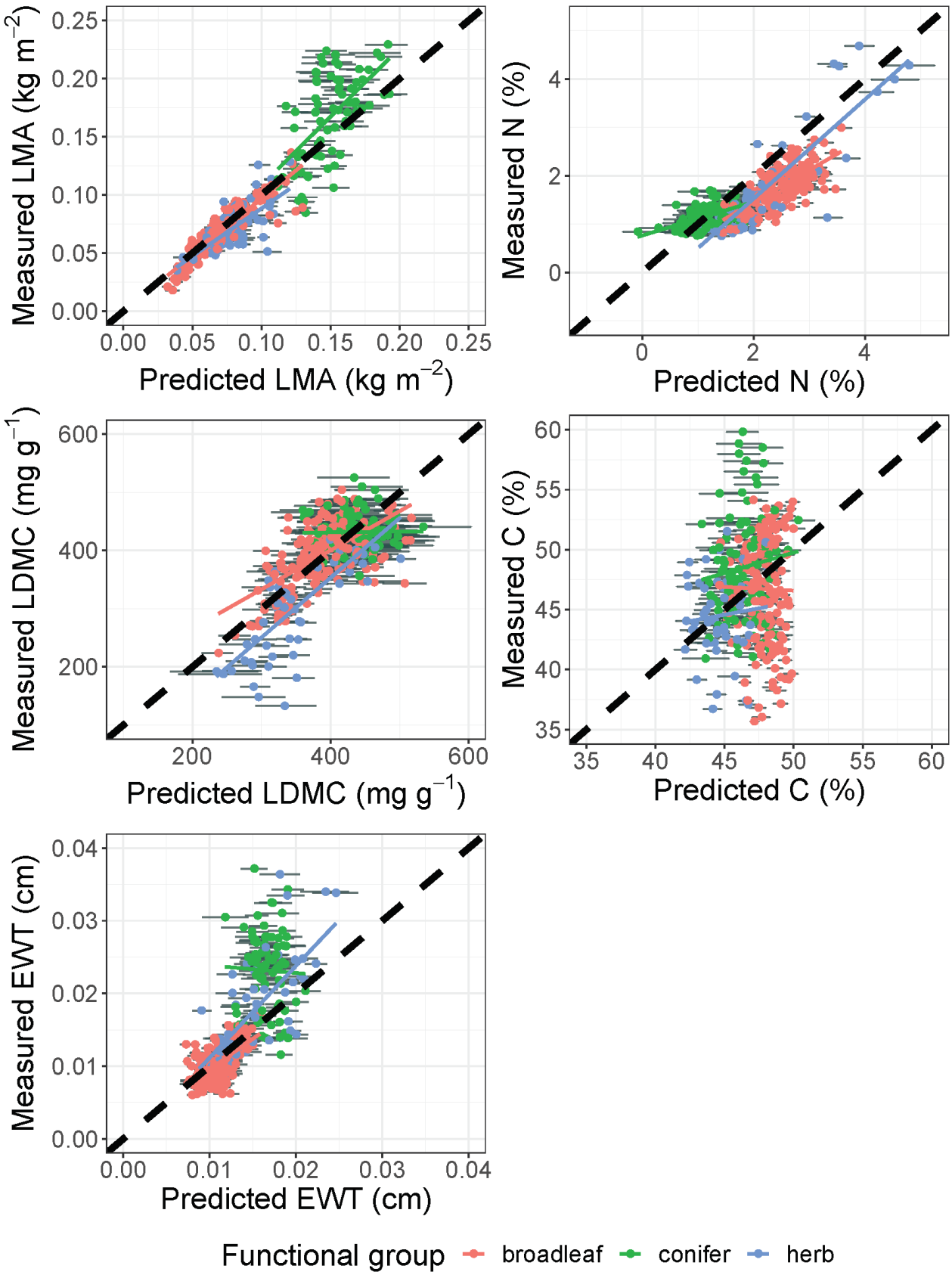
Fig. S15: External validation results for predictions of various traits in Cedar Creek data based on models trained on CABO data, restricted to 1300-2500 nm. Each panel is displayed as in Figs. S2-8.